Enhancing nucleotide metabolism protects against mitochondrial dysfunction and neurodegeneration in a *PINK1* model of Parkinson's disease

Roberta Tufi[1], Sonia Gandhi[2], Inês P. de Castro[1], Susann Lehmann[1], Plamena R. Angelova[2], David Dinsdale[1], Emma Deas[2], Hélène Plun-Favreau[2], Pierluigi Nicotera[3], Andrey Y. Abramov[2], Anne E. Willis[1], Giovanna R. Mallucci[1], Samantha H. Y. Loh[1,4] and L. Miguel Martins[1,4]

[1]MRC Toxicology Unit, Lancaster Road, Leicester LE1 9HN, UK

[2]Department of Molecular Neuroscience, Institute of Neurology, Queen Square, London WC1N 3BG, UK

[3]German Centre for Neurodegenerative Diseases (DZNE), Ludwig-Erhard-Allee 2, 53175 Bonn, Germany

[4] Corresponding authors:

L. Miguel Martins, Cell Death Regulation Laboratory, MRC Toxicology Unit, Hodgkin Building, Lancaster Road, Leicester LE1 9HN, UK, Tel + 44 116 252 5533; Fax: + 44 116 252 5616; e-mail: martins.lmiguel@gmail.com

Samantha H. Y. Loh, Cell Death Regulation Laboratory, MRC Toxicology Unit, Hodgkin Building, Lancaster Road, Leicester LE1 9HN, UK, Tel + 44 116 223 1501; Fax: + 44 116 252 5616; e-mail: shyl1@le.ac.uk

Running title: Nucleotide metabolism is neuroprotective

ABSTRACT

Mutations in *PINK1* cause early-onset Parkinson's disease (PD). Studies in *Drosophila* have highlighted mitochondrial dysfunction upon loss of Pink1 as a central mechanism of PD pathogenesis. Here we show that global analysis of transcriptional changes in *Drosophila pink1* mutants reveals an upregulation of genes involved in nucleotide metabolism, critical for neuronal mitochondrial DNA synthesis. These key transcriptional changes were also detected in brains of PD patients harbouring *PINK1* mutations. We demonstrate that genetic enhancement of nucleotide salvage pathway in neurons of *pink1* mutant flies rescues mitochondrial impairment. Also, pharmacological approaches enhancing nucleotide pools reduce mitochondrial dysfunction caused by Pink1 deficiency. We conclude that loss of Pink1 evokes the activation of a previously unidentified metabolic reprogramming pathway to increase nucleotide pools and promote mitochondrial biogenesis. We propose that targeting strategies enhancing nucleotide synthesis pathways may reverse mitochondrial dysfunction and rescue neurodegeneration in PD and, potentially, other diseases linked to mitochondrial impairment.

Keywords: *Drosophila*; mitochondria; Parkinson's disease; *PINK1*; *parkin*; stress; nucleotide metabolism; deoxyribonucleosides; folic acid

INTRODUCTION

The role of mitochondrial impairment in Parkinson's disease (PD) has long been debated. Recently, the identification of causative mutations in *PINK1,* a gene encoding a mitochondrial kinase in PD patients has renewed interest in the role of mitochondrial damage in PD [1].

Cells have evolved several lines of defence to cope with damaged mitochondria [2]. Molecular quality control represents the first level of the mitochondrial defence mechanism. This involves the upregulation of nuclear genes that encode for mitochondrial chaperones and proteases that remove misfolded and non-assembled polypeptides in mitochondria, a form of mitochondrial retrograde signalling that is commonly referred to as the mitochondrial unfolded protein response (UPR^{mt}) [3].

Invertebrates such as *Drosophila* have recently emerged as powerful model systems to study the mechanisms of PD-associated neurodegeneration. These models are also excellent *in vivo* systems for the testing of therapeutic compounds [4].

Previously, we observed that *Drosophila pink1* mutants display significant upregulation of key markers of the UPR^{mt} [5]. To extend these observations, here we proceeded with an unbiased identification of upregulated transcripts in *pink1* mutant flies.

By combining transcriptional and metabolic profiling, we have uncovered significant alterations in the nucleotide metabolism networks of *pink1* mutant flies. In the cell, two metabolic pathways, referred to as the *de novo* and salvage pathways, are involved in nucleotide metabolism. Postmitotic cells such as neurons are reported to lack the *de novo* biosynthetic pathways for nucleotide generation and instead rely on the salvage pathway [6]. The conversion of deoxyribonucleosides (dNs) to their monophosphate forms is the rate-limiting step in the salvage pathway [7], and is

catalysed by deoxyribonucleoside kinases (dNKs). *Drosophila dNK* is a highly efficient and multi-substrate single deoxyribonucleoside kinase acting on the nucleotide salvage pathway [8]. Here we show that both the genetic enhancement of the nucleotide salvage pathway by overexpression of *dNK* and the pharmacological manipulation of nucleotide metabolism enhance mitochondrial biogenesis, thus suppressing mitochondrial dysfunction associated with the PD phenotypes due to Pink1 deficiency.

Enhancement of nucleotide metabolism might therefore be of therapeutic benefit in human age-related neurological disorders linked to mitochondrial dysfunction.

RESULTS

Identification of an altered metabolic signature in *pink1* mutant flies

Previous studies have demonstrated that *Drosophila pink1* mutants exhibit transcriptional upregulation of the nuclear-encoded mitochondrial chaperones *hsp-60* and *hsc-70-5*, markers of the UPR^{mt} activation [5]. To determine the full complement of transcripts that are upregulated in *pink1* mutant flies, we employed microarray technology coupled with an *in silico* analysis approach (experimental outline, Supplementary Fig. 1a). Using the RankProducts (RP) method to identify differentially expressed genes [9] and by selecting a relaxed false discovery rate (FDR) of 50%, we detected a large number of upregulated transcripts in *pink1* mutants (Supplementary Table 1). We next employed iterative Group Analysis (iGA) [10] to identify functional classes of genes that were significantly upregulated in mutant flies (Supplementary Fig. 1b and Supplementary Table 2). This approach confirmed the upregulation of stress-related genes that code for chaperones previously detected in

pink1 mutants [5]. Interestingly, we also identified the upregulation of components of the glycine cleavage system (GCS), a mitochondrial enzymatic complex involved in glycine catabolism [11], and the upregulation of genes that belong to the purine biosynthetic pathway. Glycine catabolism is directly related to purine biosynthesis because glycine provides the C4, C5 and N7 atoms to the purine ring. Next, through network analysis, we uncovered an enrichment for components involved in glycine catabolism and folate metabolism in *pink1* mutant flies (Supplementary Fig. 1c and Supplementary Tables 3 and 4). This combined approach identified groups and networks of genes that were positively regulated in *pink1* mutants and belong to metabolic pathways related to nucleotide biosynthesis. We then sought to confirm the upregulation of components of both the *de novo* and salvage nucleotide synthesis pathways in *pink1* mutant flies. We detected a significant increase in components of the *de novo* nucleotide biosynthesis pathway, related to glycine, serine and folate metabolism. Importantly, we also confirmed the upregulation of *deoxyribonucleoside kinase* (*dNK*), a master regulator of the salvage pathway of nucleotide synthesis (Fig. 1a).

To investigate whether the observed upregulation of these genes reflects an altered metabolic state, we analysed the global metabolic changes in *pink1* mutants. This revealed that approximately 60% of the measured biochemicals are significantly altered in *pink1* mutants (Fig. 1b and Supplementary Table 5). We observed a clear decrease in the majority of tricarboxylic acid (TCA) cycle metabolites and increases in α-ketoglutarate, glutamate and glutamine. Glutamate can be converted to α-ketoglutarate through glutaminolysis, thereby compensating for losses of the TCA cycle (Reviewed in Hassel[12]). In addition, glutamine is an important source of nitrogen for purine and pyrimidine synthesis.

This analysis also revealed significant increases in metabolites that are associated with nucleotide catabolism, such as nucleoside cytidine, and salvage, such as pyrophosphate. These data led us to hypothesise that upon mitochondrial dysfunction caused by the loss of Pink1 activity, cells attempt to enhance the nucleotide pool to compensate for mitochondrial impairment.

Deoxyribonucleoside kinase enhances mitochondrial function by promoting organellar biogenesis.

To test the hypothesis that the enhancement of nucleotide pools is a compensatory mechanism following mitochondrial dysfunction, we decided to manipulate the expression of *dNK*, the rate-limiting enzyme in the nucleotide salvage pathway. *dNK* expression is upregulated in *pink1* mutants (Fig. 1a and Supplementary Table 1) and enhanced expression of *dNK* is associated with mitochondrial biogenesis[13].

We first noted that the ubiquitous expression of *dNK* led to a specific increase in mitochondrial DNA (mtDNA) (Figs. 2a, b), accompanied by an increase in mitochondrial proteins (Fig. 2c), suggesting that *dNK* expression increased mitochondrial mass in flies. This also resulted in a significant increase in the oxygen consumption (Fig. 2d and Supplementary Fig. 2a).

Mitochondrial biogenesis is achieved by the coordinated regulation of different gene subsets by the PPARγ coactivator -1α (PGC-1α) that promotes the nuclear respiratory factor 1 (NRF-1) dependent transcriptional upregulation of nuclear-encoded mitochondrial proteins. We found that *dNK* promotes an increase in both the mRNA levels of *Spargel*, the orthologue of the *PGC-1* family as well as the nuclear-encoded mitochondrial proteins Tfam, mtTFB1 and mtTFB2 (Fig. 2e). After confirming the upregulation of the Tfam protein levels (Fig. 2f), we decided to test the effects of its

loss for the dNK-dependent mtDNA increase by downregulating *Tfam* expression using RNA interference (Fig. 2g). *Tfam* knockdown alone resulted in mtDNA depletion (Tfam-RNAi#2 line) and, in *dNK* expressing flies, it abolished the dNK-induced mtDNA increase (Fig. 2h), indicating a requirement for Tfam in the dNK-dependent induction of mitochondrial biogenesis.

This biogenesis was reflected in elevated ATP levels (Fig. 2i) and in the generalised increase in the locomotor activity of flies expressing *dNK* (Figs. 2j, k and Supplementary Fig. 2b). *dNK* expressing flies have a modest decrease in lifespan (Supplementary Fig. 2c) but an increase in survival when challenged with mitochondrial poisons (Supplementary Figs. 2d, e), and also associated with enhanced levels of mitochondrial ROS detoxification components such as the superoxide dismutases 1 and 2 (SOD1 and SOD2) (Supplementary Fig. 2f).

Expression of deoxyribonucleoside kinase rescues mitochondrial dysfunction in *pink1* mutant flies

We next tested the effects of inducing mitochondrial biogenesis in *pink1* mutants by overexpressing *dNK*. Global metabolic analysis revealed that dNK promoted increases in glucose, glucose-6-phosphate (G6P) as well as the levels of the TCA cycle intermediates (Fig. 3a and Supplementary Table 6), indicating that *dNK* expression induced a partial recovery of mitochondrial metabolism. We also observed an increase in the level of the dNK substrate deoxyguanosine. Further analysis revealed that *dNK* expression rescued the loss of mtDNA (Fig. 3b), mitochondrial proteins (Fig. 3c and Supplementary Fig. 3a) and ATP (Fig. 3d) and reversed the respiration defects (Fig. 3e and Supplementary Fig. 3b) of *pink1* mutants. *dNK* expression also resulted in the significant suppression of motor impairment in *pink1* mutants (Fig. 3f), in the

recovery of mitochondrial cristae fragmentation defects in the indirect flight muscle (Fig. 3g and Supplementary Fig. 3c), in the significant reduction of crushed thorax defects (Supplementary Figs. 3d, e) and in the increased resistance to antimycin toxicity (Supplementary Fig. 3f). In flies, the absence of Pink1 results in defective mitophagy linked to the accumulation of dMfn in damaged mitochondria [14]. The expression of *dNK* had no effects on the levels of dMfn in either control or *pink1* mutant flies, suggesting that the dNK-dependent increase in mitochondrial mass is not linked to defects in the removal of defective mitochondria through mitophagy (Supplementary Fig. 3g). These data suggest that ubiquitous dNK-mediated enhancement of the nucleotide salvage pathway promotes mitochondrial biogenesis and this rescues mitochondrial dysfunction in *pink1* mutants.

Neuronal expression of deoxyribonucleoside kinase reverts the phenotype of *pink1* mutants

In *Drosophila* neurons, Pink1 deficiency leads to defects in synaptic transmission [15]. Because one of the most prominent features of *pink1* mutant flies is the degeneration of the indirect flight muscle [16], we tested whether this involves a presynaptic component. First, we confirmed the upregulation of components of both the *de novo* and salvage nucleotide synthesis pathways in the heads of *pink1* mutant flies (Fig. 4a). Next, we tested the effects of the neuronal expression of *dNK* in *pink1* mutant flies. The neuronal expression of *dNK* resulted in enhancements in the respiration and ATP levels (Figs. 4b, c), an increase in the total locomotor activity (Fig. 4d) and an improved climbing performance (Fig. 4e). *Drosophila pink1* mutants exhibit a loss of dopaminergic neurons [16], the extent of which can be assessed through analysis of the expression levels of tyrosine hydroxylase (TH), an enzyme expressed in dopaminergic

neurons [17]. We detected a decrease in the TH levels in *pink1* mutants that was reversed upon the neuronal expression of *dNK* (Fig. 5a). Accordingly, the neuronal expression of *dNK* rescued the dopaminergic neuron loss in the protocerebral posterior lateral 1 (PPL1) cluster of *pink1* mutants (Fig. 5b). To test if dNK-dependent suppression of neurodegeneration in *pink1* mutants was linked to a neuronal rescue of mitochondrial function, we assessed mitochondrial mass and potential ($\Delta\psi m$) in fly brains (Supplementary Fig. 4a). We detected a decrease of both mitochondrial mass and $\Delta\psi m$ in *pink1* mutants that was reversed upon neuronal expression of *dNK* (Figs. 5c, d).

The neuronal expression of *dNK* was also sufficient to promote the recovery of defects in respiration (Fig. 5e) and ATP levels (Supplementary Fig. 4b) in *pink1* mutants. Notably, the neuronal expression of *dNK* in *pink1* mutants significantly decreased the presence of the crushed thorax phenotype (Fig. 5f), improved climbing performance (Fig. 5g) and suppressed flight defects (Supplementary Fig. 4c). Also, neuronal expression of *pink1* was sufficient to suppress mitochondrial cristae fragmentation defects in the indirect flight muscle of *pink1* mutants (Supplementary Fig. 4d). These effects indicate that the neuronal rescue of mitochondrial function in *pink1* mutants is sufficient to suppress indirect flight muscle degeneration and motor impairment. Parkin acts as a downstream effector of PINK1 as highlighted in a series of studies in *Drosophila*, which demonstrated that the expression of *parkin* rescues the phenotype of *pink1* mutant flies[16, 18]. To test the epistatic relationship between *parkin* and *dNK*, we determined whether the neuronal expression of *dNK* could also rescue the phenotype of *parkin* mutants. We detected a decrease of $\Delta\psi m$ in *parkin* mutants that was reversed upon neuronal expression of *dNK* (Supplementary Fig. 5a). Also, the neuronal expression of *dNK* was sufficient to rescue the neurodegeneration

(Supplementary Fig. 5b), the presence of the crushed thorax phenotype (Supplementary Fig. 5c) and the degree of mitochondrial cristae fragmentation defects in the indirect flight muscle (Supplementary Fig. 5d) of *parkin* mutants.

Deoxyribonucleosides and folate stimulate mitochondrial biogenesis and suppress mitochondrial dysfunction in *pink1* mutant flies

Our findings show that in the context of reduced dNK substrate availability (Fig. 1b), *pink1* mutant flies attempt to compensate for mitochondrial stress by inducing the expression of *dNK*. To investigate the effects of enhancing the availability of dNK substrates in *pink1* mutants, we exposed the mutants to a diet supplemented with a mixture of the four major deoxyribonucleosides (dNs): deoxyadenosine (dA), deoxythymidine (dT), deoxycytidine (dC) and deoxyguanosine (dG). We found significant changes in approximately 37% of the biochemicals detected in mutant flies raised on food supplemented with all four dNs (Supplementary Table 7). Dietary dNs promoted increases in the dNK substrate 2'-deoxyguanosine, 2'-deoxyinosine and thymine, and led to an increase in biochemical intermediates of nucleotide metabolism (Supplementary Table 7 and Fig. 6a).

Upon loss of Pink1, flies respond via transcriptional upregulation of genes of the *de novo* pathway of nucleotide biosynthesis. Because of the addition of 1-carbon units in this pathway, folic acid (FA) plays a fundamental role in nucleotide synthesis. Therefore, we reasoned that administering FA to *pink1* mutants could promote nucleotide biosynthesis and confer a protective effect on mitochondria. First, we analysed the metabolic response to feeding mutant flies with FA, and found that a FA-supplemented diet led to changes in approximately 18% of the biochemicals detected (Supplementary Table 7). As with dNs, we detected increases in biochemical

intermediates of NAD+ synthesis, as well as more subtle increases in components of purine and pyrimidine biosynthesis (Supplementary Table 7 and Fig. 6a). Taken together, these changes suggest that in the absence of Pink1, supplementation with dNs or FA leads to increases in nucleotide metabolism, in particular in the NAD+ *de novo* and salvage pathways, with a resulting increase in the NAD+ pools.

We next tested the ability of dNs and FA to suppress mitochondrial dysfunction in *pink1* mutants. Administration of either dNs or FA to *pink1* mutant adults caused an increase in mtDNA (Figs. 6b, c), mitochondrial mass (Figs. 6d, e), potential (Figs. 6f, g) and an increase in ATP levels (Supplementary Fig. 6a). Moreover, dNs or FA-supplemented diet rescued the dopaminergic neuron loss of *pink1* mutants (Figs. 6h, i). Importantly, we detected a transcriptional upregulation of Tfam, mtTFB1 and mtTFB2 (Figs. 6j, k). Again, neither dNs nor FA had an effect on the levels of dMfn (Supplementary Fig. 6b), suggesting that the main effects of these compounds in *pink1* mutants are linked to supporting mitochondrial biogenesis.

Maintaining *pink1* mutants on a dNs or FA-supplemented diet significantly reduced the appearance of defective thorax phenotype (Fig. 7b), suppressed mitochondrial cristae fragmentation defects (Fig. 7a and Supplementary Fig. 7a) and flight defects (Fig. 7c). Moreover, the sole provision of either dNs or FA to adult mutants resulted in improved climbing performance (Figs. 7d, e). We also observed that purines were more efficient in the suppression of the crushed thorax phenotype in *pink1* mutants when compared to pyrimidines (Supplementary Fig. 7b). Next we tested if dNs or FA could also rescue the phenotype of *parkin* mutants. Maintaining *parkin* mutants on a dNs or FA-supplemented diet rescued the loss of $\Delta\psi m$ (Supplementary Fig. 7c) and dopaminergic neurons (Supplementary Fig. 7d), and the indirect flight muscle defects (Supplementary Figs. 7e and 7f). Together, these results suggest that both dNs and

FA-mediated enhancement of nucleotide pools and mitochondrial biogenesis compensate for the mitochondrial dysfunction observed upon disruption of the Pink1-Parkin pathway.

Deoxyribonucleosides and folate restore mitochondrial functional impairment in *PINK1* knockdown human cells

To determine whether the transcriptional upregulation of genes involved in nucleotide metabolism observed in *pink1* mutant flies was present in PD patients carrying *PINK1* mutations, we analysed the expression of key genes in post-mortem brain tissue of patients with *PINK1* mutations. Samples were selected based on RNA quality (Supplementary Fig. 8) and the expression levels of specific mRNAs were measured. We detected an increase in the mRNA levels of genes of the *de novo* purine biosynthesis pathway, in *DHFR* and in the mitochondrial thymidine kinase 2 (*TK2*), the closest orthologue of *Drosophila dNK* (Fig. 8a).

We next tested whether the exogenous supply of either dNs or FA could modulate mitochondrial bioenergetics and function in PINK1-knockdown (KD) cells. Pre-incubation of PINK1 KD cells with either dNs (Fig. 8bi) or FA (Fig. 8bii) led to a significant recovery in the TMRM signal, indicating that both treatments can rescue the loss of basal $\Delta\psi m$ resulting from a deficiency of PINK1 in human cells.

As a result of complex V maintaining the $\Delta\psi m$ in PINK1 KD cells [19], inhibition of complex V by oligomycin results in a rapid mitochondrial depolarisation and a decrease in TMRM fluorescence (Fig. 8ci), that was reversed by dNs or FA (Fig. 8c). Incubation of cells with dNs or FA resulted in minimal depolarisation of the mitochondrial membrane potential in response to oligomycin and rapid depolarisation in response to complex I inhibition by rotenone (Figs. 8cii and 8ciii). This data

suggests that dNs and FA are able to improve respiration sufficiently in order to maintain the mitochondrial membrane potential, and thus also enable complex V to function as an ATP synthase rather than an ATPase.

The redox state of the complex I substrate NADH is a function of both respiratory chain activity and the rate of substrate supply. Human PINK1 KD cells show a shift towards a more oxidised redox state [19]. To determine the effects of dNs and FA on the redox state of NADH, we measured the resting level of NADH autofluorescence and generated the "redox index", a ratio of the maximally oxidised (response to 1 μM FCCP) and maximally reduced (response to 1 mM NaCN) signals. The exogenous supply of both dNs and FA restored the basal NADH level in PINK1 KD neuroblastoma cells to values equivalent to those in the controls (Figs. 8d, e). Restoration of the NADH pool by dNs and FA would improve availability of NADH to complex 1, resulting in improved respiration and the switch to normal maintenance of the mitochondrial membrane potential by the ETC, and ATP synthesis by complex V.

DISCUSSION

Mitochondria operate a sensitive feedback system, the retrograde response, to adjust their performance [20]. This was originally discovered in yeast [21], and is a pathway of communication from mitochondria to the cell nucleus. We now show that there is an additional, previously uncharacterised, branch of the retrograde response that is activated upon mitochondrial stress along with the UPR^{mt}. Together, these two retrograde signalling branches act to alleviate stress via metabolic readjustments, promoting mitochondrial function and rescuing neurons.

Our data shows that in *pink1* mutant flies, mitochondrial dysfunction results in the transcriptional upregulation of a subset of previously unidentified genes affecting key nucleotide metabolic processes, suggesting that these processes are needed for the response to Pink1 deficiency and to protect against its neurotoxic consequences. Although the nucleotide salvage pathway, which provides deoxyribonucleotides for the DNA precursors used in DNA repair or mtDNA replication, is well known to have a role in neuronal function, to our knowledge, its role in neurodegeneration has not been reported. We have shown that genetic and pharmacological manipulation of the nucleotide metabolism pathways reverses the phenotype of *pink1* mutant flies. Thus, we have identified the enhancement of nucleotide metabolism pathways as a potential strategy to improve mitochondrial function in flies and human cells.

We propose that the ability to modulate the mitochondrial function using dNs pools or folic acid might provide important avenues for neuroprotective therapy for PD and, more broadly, for other age-related neurodegenerative diseases associated with mitochondrial dysfunction. Folic acid is a widely used dietary supplement in humans, and its safety is well established. The pharmacological manipulation of both the salvage and *de novo* pathways identified metabolites that were capable of suppressing the pathophysiological hallmarks of Pink1 dysfunction, raising the possibility of developing approaches for the protection against pathologies associated with mitochondrial dysfunction. Importantly, the concept of employing pharmacological approaches to suppress mitochondrial pathologies linked to Pink1 dysfunction was recently supported by a study showing that vitamin K_2 rescues mitochondrial impairment in *pink1* mutant flies [22].

Our data support the therapeutic potential of folic acid to enhance nucleotide pools, promoting mitochondrial biogenesis and improving mitochondrial function in neurons

in neurodegenerative disease and confirm a mechanism by which this acts. Based on our findings, we propose that a high folic acid diet might be beneficial to modulate the pathogenesis of PD by repressing mitochondrial dysfunction, opening a promising avenue towards exploring the role of folic acid in the prevention and therapy for neurodegenerative diseases like PD.

FIGURE LEGENDS

Figure 1. Loss of Pink1 results in a metabolic stress response.

RNA and metabolites were isolated from 3-day-old control and *pink1* male flies. (**a**) Quantitative RT-PCR validation for a subset of genes found to be upregulated in the microarray analysis of *Drosophila pink1* mutants and that encode for metabolic enzymes. Circled numbers are related to the metabolic reactions shown in **b**. Data are shown as the mean ± SEM, n = 3-7 per genotype, asterisks, two-tailed unpaired *t* test. See also Supplementary Fig. 1 and Supplementary Tables 1-3, and 9 for statistics source data. (**b**) Coordinated changes in metabolite abundance upon loss of *pink1* function. On the left, the relative levels of selected metabolites in *pink1* mutant flies, detected through GC-MS and LC-MS/MS analysis. A schematic diagram is shown in which these metabolites are depicted with respect to the selected upregulated transcripts. Orange and cyan correspond to metabolites that are respectively upregulated and downregulated to a significant level. The statistical significance was determined using Welch's Two Sample *t*-test (n = 8). See also Supplementary Fig. 1 and Supplementary Tables 4 and 5.

Figure 2. dNK enhances mitochondrial function by promoting organellar biogenesis.

(**a**) Enhanced mtDNA synthesis in *dNK* transgenic flies. DNA synthesis was assessed using a BrdU assay (mean ± SEM, n = 12, asterisks, two-tailed paired *t* test). (**b**) *dNK* flies show an increase in mtDNA. The ratio of mtDNA to nDNA was measured by real-time PCR using third instar larvae and 2-day-old flies with the indicated genotypes (mean ± SD, n = 9, asterisks, two-tailed paired *t* test). (**c**) *dNK* flies show

an increase in mitochondrial OXPHOS proteins. Immunoblot of samples prepared from whole 2-day-old males. α-tubulin, loading control. (**d**) Enhanced respiration in *dNK* flies. Data are shown as the mean ± SD (n = 3 per genotype, asterisks, two-tailed unpaired *t* test). (**e**) *dNK* flies show a transcriptional upregulation of *PGC-1* family homologue *Spargel* and the nuclear-encoded mtDNA binding proteins Tfam, mtTFB1 and mtTFB2. Data are shown as the mean ± SEM (n = 3-7 per genotype, asterisks, two-tailed unpaired *t* test). (**f**) dNK expression increases protein levels of mtTFA. Lysates prepared from adult flies were subjected to western blot analysis with the indicated antibodies. (**g**) RNAi-mediated suppression of *Tfam*. Expression levels were measured by real-time PCR (relative mean Ct ± SEM, n = 3-6 per genotype). Statistically significant values relative to the control are indicated (one-way ANOVA with Bonferroni's multiple comparison test). (**h**) Tfam is required for the dNK-mediated increase in mtDNA. The ratio of mtDNA to nDNA was measured by real-time PCR using 2-day-old flies with the indicated genotypes (mean ± SEM, n = 3-6 per genotype, asterisks, one-way ANOVA with Bonferroni's multiple comparison test, *** $p< 0.0001$). (**i**) *dNK* expression results in a generalised ATP increase in both young (2-day-old) and old (40-day-old) flies. Data are shown as the mean ± SD from three independent experiments (n = 3 per genotype, asterisks, two-tailed paired *t* test). (**j**) Ubiquitous expression of *dNK* enhances locomotor activity. 16 flies were tested for each genotype. (**k**) Ubiquitous expression of *dNK* enhances climbing ability. Flies were tested using a standard climbing assay (mean ± SEM, n = 100 flies per genotype, asterisks, two-tailed unpaired *t* test). See also Supplementary Figures 2 and 9, and Supplementary Table 9 for statistics source data of (**d**), (**e**), (**g**), (**h**) and (**i**).

Figure 3. Mitochondrial dysfunction in *Drosophila pink1* mutants is complemented by *dNK*.

(**a**) Expression of *dNK* partially reverses metabolic shifts in *pink1* mutants. Orange and cyan correspond to metabolites that are respectively upregulated and downregulated to a significant level. The statistical significance was determined using Welch's Two Sample *t*-test (n = 8). See also Supplementary Table 6. (**b**) *dNK* expression increases mtDNA levels in *pink1* mutants. The ratio of mtDNA to nDNA was measured by real-time PCR in flies with the indicated genotypes (mean ± SD, n = 6 per genotype, asterisks, one-way ANOVA with Bonferroni's multiple comparison test). (**c**) Expression of *dNK* restores the levels of mitochondrial respiratory complexes in *pink1* mutants. Whole-fly lysates were analysed by western blot analysis using the indicated antibodies. (**d**) *dNK* expression rescues ATP levels in *pink1* mutants. Data are shown as the mean ± SD (n = 6 per genotype, asterisks, one-way ANOVA with Bonferroni's multiple comparison test). (**e**) *dNK* expression enhances respiration in *pink1* mutants. Data are shown as the mean ± SD (n = 3 per genotype, asterisks, two-tailed unpaired *t* test). See Supplementary Table 9 for statistics source data. (**f**) *dNK* expression suppresses motor impairment in *pink1* mutants. Flies were tested using a standard climbing assay (mean ± SEM, n = 100 flies per genotype, asterisks, one-way ANOVA with Dunnett's multiple comparison test). (**g**) *dNK* expression suppresses flight muscle defects observed in *pink1* mutants. *dNK* expression rescues mitochondrial defects in *pink1* mutants (my, myofibrils; m, mitochondria; yellow outlines, mitochondria). See also Supplementary Figures 3 and 9.

Figure 4. Targeted neuronal expression of *dNK* rescues mitochondrial dysfunction in *pink1* mutants.

(**a**) Enhanced expression of components of both the *de novo* and salvage nucleotide synthesis pathways in adult heads of *pink1* mutant flies. Data are shown as the mean ± SEM (n = 3-9 in each group, asterisks, two-tailed unpaired *t* test). See Supplementary Table 9 for statistics source data. (**b**) Enhanced respiration in the heads of elav > dNK flies. Data are shown as the mean ± SEM (n = 6-8 in each genotype, asterisks, two-tailed unpaired *t* test). (**c**) Neuronal expression of *dNK* enhances ATP levels. Data are shown as the mean ± SEM (n = 6 per sample, asterisks, two-tailed unpaired *t* test). (**d**) Neuronal expression of *dNK* enhanced locomotor activity. Data are shown as the mean ± SEM (n = 13-24 in each genotype, asterisks, two-tailed unpaired *t* test). (**e**) Neuronal expression of *dNK* enhanced climbing ability (mean ± SEM, n = 100 flies per genotype, asterisks, two-tailed unpaired *t* test). See also Supplementary Fig. 4

Figure 5. Targeted neuronal expression of *dNK* rescues neurodegeneration in *pink1* mutants.

(**a**) Neuronal expression of *dNK* restores the tyrosine hydroxylase (TH) levels in *pink1* mutants. Fly head lysates were analysed using the indicated antibodies. (**b**) Expression of *dNK* rescues the loss of dopaminergic neurons in the PPL1 cluster of *pink1* mutant flies. Data are shown as the mean ± SEM (n = 12-16 brain hemispheres per genotype, asterisks, one-way ANOVA with Bonferroni's multiple comparison test). Datasets labelled "control" and "pink1B9" are also used in Figs. 6h and 6i. (**c**) Neuronal expression of *dNK* promotes an increase in neuronal mitochondrial mass of *pink1* mutants. Mitochondrial mass was calculated as the ratio of co-localisation between the TMRM signal (mitochondria) and calcein blue (whole cells). Data are the

mean ± SEM (n = 6 per genotype, asterisks, two-tailed paired *t* test). Datasets labelled "control" and "pink1B9" are also used in Figs. 6d and 6e. (**d**) Neuronal expression of *dNK* reverses the loss of Δψm in *pink1* mutants. The Δψm is represented as percentage of control. Data are shown as the mean ± SEM (n = 7 per genotype, asterisks, two-tailed unpaired *t* test). Datasets labelled "control" and "pink1B9" are also used in Figs. 6f and 6g. (**e**) Neuronal expression of *dNK* enhances respiration in *pink1* mutants. Data are shown as the mean ± SD (n = 3-10 for each genotype, asterisks, two-tailed unpaired *t* test). Complex I and II, and complex IV were measured in coupled and uncoupled mitochondria, respectively. See Supplementary Table 9 for statistics source data. (**f**) Neuronal expression of *dNK* rescues the thoracic defects of *pink1* mutants (n = 255 for pink1B9, n = 227 for pink1B9; elav>dNK, n = 187 for pink1B9;elav>pink1), asterisks , chi-square two-tailed, 95% confidence intervals). (**g**) Neuronal expression of *dNK* rescues the motor impairment of *pink1* mutants. Mean ± SEM, n = 100 flies per genotype, asterisks, two-tailed paired *t* test, relative to pink1B9). See also Supplementary Fig. 5.

Figure 6. Dietary supplementation with deoxyribonucleosides or folic acid enhances mitochondrial function and biogenesis in *pink1* mutants.

(**a**) Dietary supplementation with deoxyribonucleosides (dNs, 0.5 mg/ml each dN) or folic acid (4 mM) promotes an upregulation of biochemical components of nucleotide metabolism pathways in *pink1* mutants. Orange corresponds to metabolites that are upregulated to a significant level ($p < 0.05$). Orange boxes with a dashed outline correspond to comparisons with lower statistical significance ($0.05 < p < 0.10$). The statistical significance was determined using Welch's Two Sample *t*-test (n = 5). See also Supplementary Table 7.

(**b**) and (**c**) Dietary supplementation with dNs (b) or FA (c) during the adult stage promotes an increase in mtDNA. The ratio of mtDNA to nDNA was measured by real-time PCR using 2-day-old flies with the indicated genotypes (mean ± SD, n = 9 (**b**), n = 3 (**c**) per genotype). Statistically significant values are indicated by asterisks (one-way ANOVA with Bonferroni's multiple comparison test).

(**d**) and (**e**) dNs or FA promote an increase in neuronal mitochondrial mass of *pink1* mutants. Data are shown as the mean ± SEM (n = 6 for dNs, n = 7 for FA). Statistical significance is indicated by asterisks (two-tailed paired *t* test). Datasets labelled "control" and "pink1B9" are also used in Fig. 5c

(**f**) and (**g**) dNs or FA reverse the loss of Δψm in *pink1* mutants. The Δψm is represented as percentage of control. The error bars represent the mean ± SEM (n = 7). Statistical significance is indicated by asterisks (two-tailed unpaired *t* test). Datasets labelled "control" and "pink1B9" are also used in Fig. 5d.

(**h**) and (**i**) dNs or FA reverse the loss of dopaminergic neurons in the PPL1 cluster of *pink1* mutant. Data are shown as the mean ± SEM (n = 12-16 brain hemispheres in each group, one-way ANOVA with Bonferroni's multiple comparison test). Datasets labelled "control" and "pink1B9" are also used in Fig. 5b.

(**j**) and (**k**) dNs or FA promote the transcriptional upregulation of the nuclear-encoded mtDNA binding proteins Tfam, mtTFB1 and mtTFB2 in *pink1* mutants. The error bars represent SEM values (n = 3-4 per condition), and the asterisks indicate statistically significant values (two-tailed unpaired *t* test) relative to *pink1* flies on a normal diet. See also Supplementary Fig. 6 and Table 9 for statistics source data of (**c**), (**j**) and (**k**).

Figure 7. Dietary supplementation with deoxyribonucleosides or folic acid suppresses *pink1* mutant phenotypes.

(**a**) Suppression of flight muscle degeneration and mitochondrial defects in *pink1* mutants by dNs or FA. Ultrastructural analysis of the indirect flight muscles from *pink1* mutant flies raised on dNs or FA-supplemented food (my, myofibrils; m, mitochondria; yellow outlines, mitochondria). (**b**) Dietary supplementation with dNs or FA rescues the thoracic defects of *pink1* mutants. *pink1* mutants were exposed to a dNs or FA-supplemented diet after egg laying. *P*-values are indicated (chi-square two-tailed, 95% confidence intervals, n = 454 for normal diet, n = 448 for +dNs and n = 669 for +FA). (**c**) Dietary supplementation with dNs or FA rescues the flight defects of *pink1* mutants. Data are shown as mean ± SEM (n = 150 flies per condition). Statistically significant values relative to pink1B9 are indicated by asterisks (one-way ANOVA with Bonferroni's multiple comparison test). Datasets labelled "control" and "pink1B9" are also used in Supplementary Fig. 4c.

(**d**) and (**e**) Dietary supplementation with dNs or FA during adult stage rescues the motor impairment of *pink1* mutants. *pink1* mutants were exposed to a dNs or FA supplemented diet after eclosion. Flies were tested using a standard climbing assay (mean ± SEM, n = 100 flies per condition). Statistical significance is indicated (two-tailed unpaired *t* test). See also Supplementary Fig. 7.

Figure 8. An exogenous supply of deoxyribonucleosides and folic acid suppresses mitochondrial dysfunction upon loss of *PINK1* in human neuroblastoma cells.

(**a**) Genes encoding for enzymes of the purine biosynthetic and nucleotide salvage pathways are significantly upregulated in a subset of PD patients with *PINK1* mutations. Delta Ct values (ΔCt) for each of the analysed transcripts were normalised

to *GAPDH*. Means are represented by horizontal bars. *P*-values (two-tailed unpaired *t* test) relative to controls are indicated. See Supplementary Table 9 for statistics source data. (**b**) An exogenous supply of dNs (i) or folate (ii) reversed the reduction in the basal mitochondrial membrane potential in *PINK1* KD cells. Cells were grown for 24 hr in media supplemented with dNs (20 μM each dN) or FA (300 μM) and were compared to cells grown in normal media. (i) mean ± SEM, n = 240 cells of three separate clones, data from 6 independent experiments. (ii) mean ± SEM, n = 180 cells of three separate clones, data from 6 independent experiments. Statistical significance is indicated by asterisks (two-tailed paired *t* test). (**c**) The reversal of oligomycin-induced Δψm by dNs and FA. In *PINK1* KD cells (Ci), oligomycin caused marked mitochondrial depolarisation, whereas the exogenous addition of either dNs (Cii) or FA (Ciii) completely blocked depolarisation. Cells were grown for 24 hr in media supplemented with dNs (20 μM each dN) or FA (300 μM) and were compared to cells grown in normal media. Error bars represent mean ± SEM (n = 180 cells). (**d**, **e**) Reversal of the loss of NADH redox state in *PINK1* KD cells by dNs and FA. The resting level of NADH autofluorescence was measured by determining the ratio between the signal for the maximally oxidised condition (response to 1 μM FCCP) and the signal for the maximally reduced condition (response to 1 mM NaCN) to determine the baseline "redox state" in control cells (**d**i). *PINK1* KD cells showed a decreased redox state (**d**ii and **e**), whereas the exogenous supply of either dNs or FA recovered the redox state (**d**iii, **d**iv and **e**). Cells were grown for 24 hr in media supplemented with dNs (20 μM each dN) or FA (300 μM) and were compared to cells grown in normal media. The error bars represent the mean ± SEM (n = 180 cells). Statistical significance is indicated by asterisks (two-tailed paired *t* test).

ACKNOWLEDGEMENTS

We would like to thank Joël Silber, Alex Whitworth, Thomas Rival, the Vienna *Drosophila* RNAi Center and the Bloomington *Drosophila* Stock Center for fly stocks; and Jalpa Parmar for fly food preparation. We thank Doug Green for comments on the manuscript and helpful discussions. We thank Alexey Antonov for advice on advanced biostatistics. We also thank Magda Locker for helpful discussions.

CONTRIBUTIONS

A.Y.A., G.R.M., L.M.M., R.T and S.H.Y.L conceived and designed the experiments. A.Y.A., D.D., I.P.d.C., L.M.M., P.R.A., R.T., S.G., S.L. and S.H.Y.L. performed the experiments and analysed the data. E.D. contributed materials. A.E.W., H.P-F. and P.N. provided experimental and conceptual advice. G.R.M., L.M.M., R.T., S.G. and S.H.Y.L wrote the paper. S.H.Y.L. and L.M.M. contributed equally as joint last authors.

CONFLICT OF INTEREST

The authors declare no conflict of interest.

REFERENCES

1. Deas, E., Plun-Favreau, H. & Wood, N.W. PINK1 function in health and disease. *EMBO molecular medicine* **1**, 152-165 (2009).
2. Tatsuta, T. & Langer, T. Quality control of mitochondria: protection against neurodegeneration and ageing. *EMBO J* **27**, 306-314 (2008).
3. Broadley, S.A. & Hartl, F.U. Mitochondrial stress signaling: a pathway unfolds. *Trends Cell Biol* **18**, 1-4 (2008).
4. Lu, B. & Vogel, H. Drosophila models of neurodegenerative diseases. *Annu Rev Pathol* **4**, 315-342 (2009).
5. Pimenta de Castro, I. *et al.* Genetic analysis of mitochondrial protein misfolding in Drosophila melanogaster. *Cell death and differentiation* **19**, 1308-1316 (2012).
6. Arner, E.S. & Eriksson, S. Mammalian deoxyribonucleoside kinases. *Pharmacol Ther* **67**, 155-186 (1995).
7. Curbo, S., Amiri, M., Foroogh, F., Johansson, M. & Karlsson, A. The Drosophila melanogaster UMP-CMP kinase cDNA encodes an N-terminal mitochondrial import signal. *Biochemical and biophysical research communications* **311**, 440-445 (2003).
8. Munch-Petersen, B., Piskur, J. & Sondergaard, L. Four deoxynucleoside kinase activities from Drosophila melanogaster are contained within a single monomeric enzyme, a new multifunctional deoxynucleoside kinase. *The Journal of biological chemistry* **273**, 3926-3931 (1998).
9. Breitling, R., Armengaud, P., Amtmann, A. & Herzyk, P. Rank products: a simple, yet powerful, new method to detect differentially regulated genes in replicated microarray experiments. *FEBS Lett* **573**, 83-92 (2004).
10. Breitling, R., Amtmann, A. & Herzyk, P. Iterative Group Analysis (iGA): a simple tool to enhance sensitivity and facilitate interpretation of microarray experiments. *BMC Bioinformatics* **5**, 34 (2004).
11. Kikuchi, G., Motokawa, Y., Yoshida, T. & Hiraga, K. Glycine cleavage system: reaction mechanism, physiological significance, and hyperglycinemia. *Proc Jpn Acad Ser B Phys Biol Sci* **84**, 246-263 (2008).
12. Hassel, B. Carboxylation and anaplerosis in neurons and glia. *Mol Neurobiol* **22**, 21-40 (2000).
13. Icreverzi, A., de la Cruz, A.F., Van Voorhies, W.A. & Edgar, B.A. Drosophila cyclin D/Cdk4 regulates mitochondrial biogenesis and aging and sensitizes animals to hypoxic stress. *Cell Cycle* **11**, 554-568 (2012).
14. Ziviani, E., Tao, R.N. & Whitworth, A.J. Drosophila parkin requires PINK1 for mitochondrial translocation and ubiquitinates mitofusin. *Proc Natl Acad Sci U S A* **107**, 5018-5023 (2010).
15. Morais, V.A. *et al.* Parkinson's disease mutations in PINK1 result in decreased Complex I activity and deficient synaptic function. *EMBO Mol Med* **1**, 99-111 (2009).
16. Park, J. *et al.* Mitochondrial dysfunction in Drosophila PINK1 mutants is complemented by parkin. *Nature* **441**, 1157-1161 (2006).
17. Wills, J. *et al.* Elevated tauopathy and alpha-synuclein pathology in postmortem Parkinson's disease brains with and without dementia. *Experimental neurology* **225**, 210-218 (2010).

18. Clark, I.E. *et al.* Drosophila pink1 is required for mitochondrial function and interacts genetically with parkin. *Nature* **441**, 1162-1166 (2006).
19. Gandhi, S. *et al.* PINK1-associated Parkinson's disease is caused by neuronal vulnerability to calcium-induced cell death. *Mol Cell* **33**, 627-638 (2009).
20. Allen, J.F. Control of gene expression by redox potential and the requirement for chloroplast and mitochondrial genomes. *J Theor Biol* **165**, 609-631 (1993).
21. Butow, R.A. & Avadhani, N.G. Mitochondrial signaling: the retrograde response. *Mol Cell* **14**, 1-15 (2004).
22. Vos, M. *et al.* Vitamin K2 is a mitochondrial electron carrier that rescues pink1 deficiency. *Science* **336**, 1306-1310 (2012).
23. Antonov, A.V., Schmidt, E.E., Dietmann, S., Krestyaninova, M. & Hermjakob, H. R spider: a network-based analysis of gene lists by combining signaling and metabolic pathways from Reactome and KEGG databases. *Nucleic acids research* **38**, W78-83 (2010).
24. Schmittgen, T.D. & Livak, K.J. Analyzing real-time PCR data by the comparative C(T) method. *Nat Protoc* **3**, 1101-1108 (2008).
25. Antonov, A.V. BioProfiling.de: analytical web portal for high-throughput cell biology. *Nucleic acids research* **39**, W323-327 (2011).
26. Legent, K. *et al.* In vivo analysis of Drosophila deoxyribonucleoside kinase function in cell cycle, cell survival and anti-cancer drugs resistance. *Cell Cycle* **5**, 740-749 (2006).
27. Behl, B. *et al.* An ELISA-based method for the quantification of incorporated BrdU as a measure of cell proliferation in vivo. *J Neurosci Methods* **158**, 37-49 (2006).
28. de Castro, I.P. *et al.* Drosophila ref(2)P is required for the parkin-mediated suppression of mitochondrial dysfunction in pink1 mutants. *Cell Death Dis* **4**, e873 (2013).
29. Costa, A.C., Loh, S.H. & Martins, L.M. Drosophila Trap1 protects against mitochondrial dysfunction in a PINK1/parkin model of Parkinson's disease. *Cell Death Dis* **4**, e467 (2013).
30. Poole, A.C. *et al.* The PINK1/Parkin pathway regulates mitochondrial morphology. *Proc Natl Acad Sci U S A* **105**, 1638-1643 (2008).
31. Whitworth, A.J. *et al.* Increased glutathione S-transferase activity rescues dopaminergic neuron loss in a Drosophila model of Parkinson's disease. *Proc Natl Acad Sci U S A* **102**, 8024-8029 (2005).
32. Abou-Sleiman, P.M. *et al.* A heterozygous effect for PINK1 mutations in Parkinson's disease? *Ann Neurol* **60**, 414-419 (2006).
33. Schroeder, A. *et al.* The RIN: an RNA integrity number for assigning integrity values to RNA measurements. *BMC Mol Biol* **7**, 3 (2006).
34. Storey, J.D. & Tibshirani, R. Statistical significance for genomewide studies. *Proceedings of the National Academy of Sciences of the United States of America* **100**, 9440-9445 (2003).
35. Wexler, E.J. (Linda.com, Inc., Ventura; 2008).

Methods

Microarray acquisition and analysis

RNA was prepared from 3-day-old male adult flies (6 samples in total, 3 replicates for each genotype). The RNA quality was confirmed using an Agilent 2100 Bioanalyzer. The target samples were prepared following the GeneChip One-Cycle Target Labeling protocol (Affymetrix). All of the samples were then hybridised to GeneChip Drosophila Genome 2.0 arrays (Affymetrix). The arrays were washed and stained using Affymetrix protocols on a Fluidics Station 400, scanned using a Gene Array Scanner 2500 and deposited at ArrayExpress under accession E-MEXP-3645. Differential expression was analysed by the UK *Drosophila* Affymetrix Array Facility (University of Glasgow, Scotland, UK) with RankProducts and iterative Group Analysis using the automated FunAlyse pipeline.

A network analysis was performed on the list of upregulated genes with an FDR below 50% using R-Spider, a web-based tool that integrates gene lists with the Reactome and KEGG databases [23].

RNA Extraction and Real-Time PCR

Isolation of total RNA was performed using the RNeasy Mini Kit (QIAGEN). Quantitative real-time RT-PCR (qRT-PCR) was performed on an Mx4000 (Stratagene) real-time cycler using the QuantiTect SYBR Green RT- PCR system (QIAGEN). Gene-specific primers were obtained from QIAGEN (QuantiTect Primer Assays) for the following genes: CG3999 (Cat. no. QT00972349), CG3011/Shmt2 (Cat. no. QT00498904), CG6415 (Cat. no. QT00934318), CG18466-RB/Nmdmc (Cat. no. QT00503153), CG14887-RA/Dhfr (Cat. no. QT00976227), CG11089/atic (Cat. no. QT00982023), CG9127-RA/ade2 (Cat. no. QT01084958), CG5452-RA/*dNK* (Cat. no. QT0097774), *actin 79B* (Cat. no. QT00967393). The relative transcript levels of each target genes were normalised against *actin* mRNA levels; quantification was performed using the comparative Ct method [24].

Metabolic profiling

Global metabolic profiles were obtained for each individual genotype using the Metabolon Platform (Metabolon Inc. NC, USA). Briefly, each sample consisted of 8 biological replicates (100 flies per replicate). The sample preparation process was carried out using the automated MicroLab STAR® system from Hamilton Company. For sample extraction, a 80% (v/v) methanol:water solution was used. Recovery standards were added prior to the first step in the extraction process for quality control purposes. Sample preparation was conducted using a proprietary series of organic and aqueous extractions to remove the protein fraction while allowing maximum recovery of small molecules. The resulting extract was divided into two fractions; one for analysis by LC and one for analysis by GC. Samples were placed briefly on a TurboVap® (Zymark) to remove the organic solvent. Each sample was then frozen and dried under vacuum. Samples were then prepared for the appropriate instrument, either LC/MS or GC/MS. Compounds above the detection threshold were identified by comparison to library entries of purified standards or recurrent unknown entities. Identification of known chemical entities was based on comparison to metabolomic library entries of purified standards.

Gene network analysis

We used R-Spider [23] to construct a single connected network based on upregulated transcripts found in *pink1* mutant flies. We first submitted a list of 1,693 upregulated genes, selected with an FDR of 50%, to the R-Spider analysis through a dialog-driven web interface [25]. From this list, we were able to connect 68 genes into a network of 92 nodes (Supplementary Fig. 1c and Table 3). We then reduced the FDR threshold to 5% to obtain a list of network components below this threshold.

Genetics and *Drosophila* strains

Fly stocks and crosses were maintained on standard cornmeal agar media at 25°C. The strains used were UAS-*dNK* [26], *pink1*^{B9} [16], *park*^{25}, UAS-*pink1* and UAS-*parkin* (kind gifts from A. Whitworth, MRC, Centre for Developmental and Biomedical Genetics, University of Sheffield, Sheffield, UK), *da*-GAL4 and *elav*-GAL4 (Bloomington *Drosophila* Stock Center), and Tfam RNAi line (Transformant ID: 107191, Vienna Drosophila RNAi Center). The genotypes for all of the flies used in this study are listed in Supplementary Table 8. For crosses to combine *pink1*^{B9} mutants with GAL4/UAS transgenes, paternal males with marked X chromosome (y- or FM6) were used to allow for the correct identification of *pink1*^{B9} mutant progeny. The deletion of *pink1* coding region (570bp, as described in [16]) and the loss of *pink1* mRNA were routinely detected using PCR and qRT-PCR, respectively.

BrdU ELISA in *Drosophila* adult tissues

Assessment of mtDNA synthesis was performed using a BrdU ELISA assay. After 40 hr of exposure to food containing 50 mM BrdU (SIGMA, Cat. no. B5002), individual adult males were anaesthetised and immediately homogenised in 400 µl of chilled homogenisation buffer (0.25 M sucrose, 10 mM EDTA, 30 mM Tris-HCl, pH 7.5). After 10 minutes of incubation on ice, lysates were centrifuged at 2700 rpm (700 x g) at 4°C for 5 minutes. Supernatants were then transferred into fresh tubes and centrifuged at 10400 rpm (10,000 x g) at 4°C for 30 minutes. The supernatants were discarded, and mitochondrial pellets were resuspended in 30 µl of 100 mM Tris-HCl, pH 8.5, containing 5 mM EDTA, 0.2% (w/v) SDS, 200 mM NaCl and 100 µg/ml proteinase K. The samples were kept on ice for 10 minutes and incubated at 55°C in a thermal mixer for 3 hr. After centrifugation at max speed, the supernatants were recovered and 100 µl of absolute ethanol was added. The samples were mixed and kept at -20 °C for at least 10 minutes (up to 16 hr).

After centrifugation at max speed, the resulting mitochondrial pellets were dried and resuspended in PBS containing 0.1% BSA. Following denaturation at 98°C for 30 minutes, samples were immediately placed at 4°C and loaded (100 µl/well) onto a 96-well microtiter plate (MaxiSorb, Nunc). The BrdU ELISA was performed according to [27].

Quantification of mtDNA

Analysis of the mtDNA content was performed by quantitative real-time PCR as previously described [28].

ATP assays

Five thoraces (or whole flies, or eleven heads, depending on the experiment) from 2 day-old flies were dissected and processed as previously described [29].

Respirometry Analysis

Mitochondrial respiration was assayed at 37° C by high-resolution respirometry as previously described [29].

Behavioural Analysis

For the climbing assay, 10 male flies at the indicated age were placed into glass columns (23 cm long, 2.5 cm in diameter) that were lined with nylon mesh (250 microns, Dutscher Scientific) and marked with a line at 15 cm. After a 30-60 minute recovery from CO_2 anaesthesia, flies were gently tapped to the bottom of the vial, and the time required for 5 flies to climb above the marked line was recorded. For each experiment, at least three cohorts of 10 flies from each genotype were scored, and all of the experiments were performed in triplicate. For the locomotor assay, male flies were individually placed in *Drosophila* Activity Monitoring System (DAMS; TriKinetics, Waltham, MA, USA) testing chambers (capped with standard cornmeal agar media at one end). The flies were grown in a light/dark 12 hr:12 hr cycle at 25°C. Data were exported into Excel, and the average total locomotor activity (as measured by the total number of recorded midline crossings per hr) was calculated for each genotype (n = 16 per genotype). All of the experiments were performed in triplicate. Flight assays were performed as previously described [22]. These flight assays are likely to have different sensitivities when compared to other approaches [16, 30].

Data acquired for the assessment of both genetic and pharmacological rescue of either *pink1* or *parkin* mutants were obtained as a single experimental set before statistical analysis

Longevity assays

Groups of 10 newly eclosed males of each genotype were placed into separate vials with food and maintained at 25°C. Flies were transferred into vials containing fresh food every 2 to 3 days, and the number of dead flies was recorded. Data are presented as Kaplan-Meier survival distributions, and the significance was determined by log-rank tests.

Electron Microscopy

This was performed as previously described [28].

Antibodies

Primary antibodies employed in this study were OXPHOS rodent cocktail, and NDUFS3/complexI 1:1000 (Mitosciences), mtTFA (TFAM) 1:1000 (Abcam, ab47548), Tyrosine Hydroxylase (TH) 1:1000 (Millipore), α-tubulin 1:5000 (SIGMA), SOD1 1:1000 (SOD-100, Stressgen), SOD2 1:1000 (SOD-110, Stressgen), dMfn 1:1000 (a kind gift from A. Whitworth, MRC, Centre for Developmental and Biomedical Genetics, University of Sheffield, Sheffield, UK).

Protein extraction and western blotting

Protein extracts from whole flies or heads were prepared by grinding flies in lysis buffer (25 mM Tris-HCl pH 7.4, 300 mM NaCl, 5 mM EDTA, 1 mM PMSF, 0.5% (w/v) Nonidet-40) containing the protease inhibitors leupeptin, antipain, chymostatin, pepstatin (SIGMA) at manufacturer's recommended dilution. The suspensions were cleared by centrifugation at 15700 x g for 10 minutes at 4°C and protein

concentrations of the supernatants were estimated using the Bradford assay (Bio-Rad). After adding 10% (w/v) SDS, aliquots of each fraction were mixed with 2 X SDS loading buffer. For SDS-PAGE equivalent amounts of proteins were resolved on 10% Precast Gels (Invitrogen) and transferred onto nitrocellulose membranes. The membranes were blocked in TBS (0.15 M NaCl, 10 mM Tris-HCl [pH 7.5]) containing 5% (w/v) dried nonfat milk (blocking solution) for 1 hr at room temperature, probed with the indicated primary antibody before being incubated with the appropriate HRP-conjugated secondary antibody. Antibody complexes were visualized by Pierce enhanced chemiluminescence (ECL).

Microscopy-based assessment of mitochondrial function and density

For measurements of $\Delta\psi m$ in fly brains, these were loaded for 40 min at room temperature with 40 nM tetramethylrod- amine methylester (TMRM) in loading buffer (10 mM HEPES pH 7.35, 156 mM NaCl, 3 mM KCl, 2 mM $MgSO_4$, 1.25 mM KH_2PO_4, 2 mM $CaCl_2$, 10 mM glucose) and the dye was present during the experiment. In these experiments, TMRM is used in the redistribution mode to assess $\Delta\psi m$, and therefore a reduction in TMRM fluorescence represents mitochondrial depolarization. Confocal images were obtained using a Zeiss 710 CLSM equipped with a 40× oil immersion objective. Illumination intensity was kept to a minimum (at 0.1–0.2% of laser output) to avoid phototoxicity and the pinhole set to give an optical slice of 2 μm. Fluorescence was quantified in individual mitochondria by exciting TMRM using the 565 nm laser and fluorescence measured above 580 nm. Z-stacks of 4-5 fields per brain were acquired, and the mean maximal fluorescence intensity was measured for each group. The differences in $\Delta\psi m$ are expressed as a percentage compared to control brains (taken as 100%). Mitochondrial mass was calculated as percentage of co-localisation of the TMRM fluorescence (mitochondria) and calcein blue (whole neurons). Brains were loaded with 40 nM TMRM and 5 μM calcein blue am for 40 min at room temperature in loading buffer. Calcein blue was excited using the 405 nm laser and fluorescence measured above 430 nm. Data acquired for the assessment of both genetic and pharmacological rescue of either *pink1* or *parkin* mutants were obtained as a single experimental set before statistical analysis.

For measurements of $\Delta\psi m$ in human neuroblastoma cells, these were loaded with 25 nM TMRM for 30 min at room temperature, and the dye was present during the experiment. TMRM is used in the redistribution mode to assess $\Delta\psi m$ in individual mitochondria, and therefore a reduction in TMRM fluorescence represents mitochondrial depolarization. NADH autofluorescence was excited at 351 and measured at 375–470 nm.

Analysis of Dopaminergic neurons

Fly brains were dissected from 20-day-old flies and stained for anti-tyrosine hydroxylase (Immunostar Inc.) as described previously [31]. Brains were mounted on Vectashield (Vector Laboratories), imaged by confocal microscopy and TH-positive PPL1 cluster neurons were counted. Data acquired for the assessment of both genetic and pharmacological rescue of either *pink1* or *parkin* mutants were obtained as a single experimental set before statistical analysis.

Oxidative stress assay

The procedure used for longevity assay, was repeated for oxidative stress assays using food containing paraquat or antimycin at the indicated concentration. Data are

presented as Kaplan-Meier survival distributions and significance determined by log-rank tests.

Analysis of post-mortem human samples

Flash frozen post-mortem brain tissue was obtained from the Queen Square Brain Bank (QSBB) after acquiring ethical approval from National Hospital of Neurology and Neurosurgery (NHNN), Local Research Ethics Committee (LREC) and Research and Development department of University College Hospital London (UCLH). Informed consent had been acquired by the QSBB. All the tissue had Caucasian ancestry. Three flash-frozen post-mortem brains with classical neuropathological appearances of Parkinson's disease, associated with heterozygous mutations in the *PINK1* gene, were originally identified in an extensive mutation screen [32]. Four flash-frozen control brains were used as age-matched and pH-matched controls. A total of 70 to 90 mg of tissue was homogenized and RNA was extracted using an RNeasy mini kit (Qiagen, UK) according to the manufacturer's protocol. Briefly, 1 ml of Qiazol was added to a 90 mg sample, and the mixture was homogenized using a Qiagen TissueRuptor with disposable probes for cell lysis. After homogenization, 200 µl chloroform was added and the mixture mixed. The subsequent aqueous and organic layers were separated by centrifugation at 10000xg for 30 minutes at 4°C. The upper aqueous phase containing the RNA was removed and 200µl of 70% glacial ethanol added. The mixture was applied to the silica gel matrix and centrifuged at 8000xg for 15 s to allow RNA to be absorbed on to the membrane. Contaminants were washed through (8000 g for 15 s). RNA was then eluted in >50µl RNase-free H_2O and stored at -80°C. All RNA preparations were analysed on a Nanodrop ND-1000 Spectrophotometer (Thermo Scientific, Wilmington, NC, USA) to determine the RNA concentration and yield, and on an Agilent 2100 Bioanalyzer (Agilent Technologies, Berkshire, UK) using the Eukaryote Total RNA Nano Assay to determine the quality of the RNA using the RNA integrity number (RIN). The latter is a software algorithm developed by Agilent Technologies to standardize assessment of RNA quality. The algorithm is based on a number of features that denote RNA integrity, including the ratio of the two main species of ribosomal RNA (18S and 28S) and the relative height of the 28S rRNA peak. RIN of 0 indicates completely degraded or undetectable RNA and RIN of 10 indicates intact RNA with no degradation [33].

Quantitative real-time RT-PCR was performed on an Mx4000 (Stratagene) real-time cycler using the QuantiTect SYBR Green RT- PCR system (QIAGEN). Gene-specific primers were obtained from QIAGEN (QuantiTect Primer Assays) for the following genes: Hs_DHFR (Cat. no. QT01668730), Hs_ATIC (Cat. no. QT00015526), Hs_PAICS (Cat. no. QT00087458), Hs_TK2 (Cat. no. QT00071428). GADPH primers were from SIGMA (Forward primer: GAAGGTGAAGGTCGGAGT; Reverse primer: GAAGATGGTGATGGGATTTC). The Ct value of each target gene was normalised by the subtraction of the Ct value from the housekeeping gene - *GADPH* – to obtain the ΔCt value. The relative gene expression level was shown as ΔCt, which is inversely correlated to gene expression level.

Statistical Analysis

Descriptive and inferential statistics analyses were performed using GraphPad Prism 5 (www.graphpad.com). Computation of the minimal sample size for the variables measured in this study was assessed by power analysis, setting alpha initially to 0.05, employing StatMate 2 (www.graphpad.com).

Data are presented as the mean values, and the error bars indicate ± SD or ± SEM, as indicated. The number of biological replicates per experimental variable (n) is indicated in the figure legends. Parametric tests were used, after confirming that the variables under analysis displayed Gaussian distributions using the D'Agostino-Pearson test (performed using data obtained from pilot experiments and computed using GraphPad Prism 5). The significance is indicated as *** for $P < 0.001$, ** for $P < 0.01$, * for $P < 0.05$. For the statistical analysis of biochemicals in flies pair-wise comparisons were performed using Welch's t-tests. The q-value provides an estimate of the false discovery rate (FDR) according to Storey and Tibshirani [34]. The investigators gathering quantitative data on biological samples were blinded to the sample identities at the time of analysis. No specific randomization strategies were employed when assigning biological replicates to treatment groups.

Digital Image Processing

Fluorescence, TEM and western blot images were acquired as uncompressed bitmapped digital data (TIFF format) and processed using Adobe Photoshop CS3 Extended, employing established scientific imaging workflows [35]. Images shown are representative of at least 3 independent experiments.

Supplementary Figures

Supplementary Figure 1. Analysis of gene networks induced upon loss of *pink1*. Related to Fig.1.

(a) Workflow employed for the identification of specific gene networks induced by loss of *pink1* function. Inputs are depicted in cyan, outputs in orange and processing steps in green. Arrows illustrate the flow of information. **(b)** Groups of functionally related genes upregulated in *pink1* mutant flies. Groups were identified by iGA. Gene ontology classes are ranked by PC-value. *P*-values were calculated using the hypergeometric distribution; rank of a particular gene in the list of differentially expressed genes is created from the RP list by exclusion of genes that are not assigned to the gene ontology classes; FDR, false discovery rate; FC, fold-change calculated as an antilog of a mean log-fold-change over all possible between-chip comparisons contributing to a given between-group comparison. See also Supplementary Table 2. **(c)** Network organization of genes upregulated in *pink1* mutant flies. A D1 network model was returned by *R* spider on submission of 1693 candidate genes found to be upregulated in *pink1* mutant flies ($p<0.005$, computed according to Antonov et al [23]). Boxes represent input genes, circles represent compounds which are common substrates or products for connected genes. Hexagons are used to specify the colour of canonical Reactome or KEGG pathway. Asterisks correspond to network components below 5% FDR threshold and thick connectors link components above such threshold. See also Supplementary Tables 3 and 4.

Supplementary Figure 2. Analysis of *dNK* expressing flies. Related to Fig. 2.

(**a**) Enhanced respiration in *dNK* expressing flies. Activity of the indicated complexes in uncoupled mitochondria was measured by high-resolution respirometry. Data are shown as the mean ± SD (n = 3-4 in each genotype). Statistically significant values relative to control (da > +) are indicated by the asterisks (two-tailed unpaired *t* test) See Supplementary Table 9 for statistic source data. (**b**) *dNK* expression enhanced locomotor activity. Quantification of locomotor activity (counted as number of midline crossings per hr) was recorded for control (da > +) and *dNK* expressing flies for a period of 260 hr, n = 16 for each genotype. The *p* value (***, $p<0.0001$) was calculated by two-tailed unpaired t-test. (**c**) *dNK* expressing flies (red) show a reduction in total lifespan, compared to controls (black). Fly viability was scored over a period of 60 days, n = 80 for da>+ and n = 138 for da>dNK. Statistical significance is indicated (log-rank, Mantel-Cox test). (**d**) *dNK* expressing flies (red) show enhanced resistance to antimycin A toxicity, compared to controls (black). Fly viability was scored over a period of 40 days, n = 30 for da>+ and n = 31 for da>dNK. Statistical significance is indicated (log-rank, Mantel-Cox test). (**e**) *dNK* expressing flies (red) show enhanced resistance to paraquat toxicity, compared to controls (black). Fly viability was scored over a period of 25 days, n = 54 for da>+ and n = 62 for da>dNK. Statistical significance is indicated (log-rank, Mantel-Cox test). (**f**) *dNK* expressing flies show enhanced levels of mitochondrial ROS detoxification components, superoxide dismutases 1 and 2 (SOD1 and SOD2). Whole-fly lysates were analysed by western blot analysis using the indicated antibodies.

Supplementary Figure 3. Mitochondrial dysfunction in *pink1* mutants is complemented by *dNK*. Related to Fig. 3.

(**a**) Expression of *dNK* restores levels of complex I subunit NDUFS3 in *pink1* mutants. Whole fly lysates were analysed using the indicated antibodies. (**b**) *dNK* expression enhances respiration in *pink1* mutants. Activity of the indicated complexes in the uncoupled mitochondria was measured by high-resolution respirometry. Data are shown as the mean ± SEM (n = 6 in each genotype). Statistically significant values are indicated by asterisks (one-way ANOVA with Bonferroni's multiple comparison test). (**c**) Percentages of indirect flight muscle mitochondria exhibiting fragmented cristae are presented for the indicated genotypes (n = 273 for control, n = 240 for pink1B9, n = 340 for pink1B9,dNK). Asterisks indicate statistical significance (chi-square, two-tailed, 95% confidence intervals) (**d**) Expression of *dNK* rescues the thoracic defects of *pink1* mutants. SEM micrographs of thoraces from flies with the indicated genotypes show that the collapsed-thorax phenotype (middle) of *pink1* mutants is suppressed by *dNK* expression (right). A control thorax (from da > +) is also shown (left). (**e**) Percentages of flies exhibiting defective thorax after eclosion are presented for the indicated genotypes (n = 400 per genotype). Asterisks indicate statistical significance relative to pink1B9 (chi-square, two-tailed, 95% confidence intervals). (**f**) *dNK* expression enhances the resistance of *pink1* mutant flies to antimycin (50μg/ml) toxicity. Fly viability was scored over a period of 40 days, n = 60 for da>+, n = 68 for pink1B9,da>+ and n = 66 for pink1B9,da>dNK. Statistical significance is indicated (log-rank, Mantel-Cox test). (**g**) Expression of *dNK* does not alter dMfn levels. Whole fly lysates were analysed using the indicated antibodies.

Supplementary Figure 4. Targeted neuronal expression of *dNK* rescues mitochondrial dysfunction in *pink1* mutant. Related to Fig. 4.

(**a**) Confocal image taken from a whole mounted *Drosophila* brain showing a neuron loaded with TMRM and calcein blue. (**b**) Neuronal expression of *dNK* enhances ATP levels in *pink1* mutants. ATP levels were measured using a bioluminescence assay. Data are shown as the mean ± SD (n = 9 in each group). Statistical significance is indicated (one-way ANOVA with Bonferroni's multiple comparison test). (**c**) Neuronal expression of *dNK, pink1 and drp1* rescues the flying ability of *pink1* mutants. (mean ± SEM, n = 150 flies per genotype). Statistically significant values relative to pink1B9 are indicated by asterisks (one-way ANOVA with Bonferroni's multiple comparison test). Datasets labelled "control" and "pink1B9" are also used in Fig. 7c. (**d**) *pink1* expression suppresses flight muscle defects observed in *pink1* mutants. Ultrastructural analysis of the indirect flight muscles showed that *pink1* expression rescues mitochondrial defects in *pink1B9* mutants (my, myofibrils; m, mitochondria; yellow outlines, mitochondria). Percentages of indirect flight muscle mitochondria exhibiting fragmented cristae are presented for the indicated genotypes (n = 185 for pink1B9, n = 340 for pink1B9;elav>pink1). Asterisks indicate statistical significance (chi-square, two-tailed, 95% confidence intervals).

Supplementary Figure 5. Targeted neuronal expression of *dNK* rescues mitochondrial dysfunction in *parkin* mutant. Related to Fig. 5.

(**a**) Neuronal expression of *dNK* reverses the loss of Δψm in *parkin* mutants. The Δψm is represented as percentage of control. Data are shown as the mean ± SEM (n = 5-7 brains per genotype). Statistical significance is indicated by asterisks (two-tailed paired *t* test). Datasets labelled "control" and "park25" are also used in Supplementary Fig. 7c. (**b**) Neuronal expression of *dNK* rescues the loss of dopaminergic neurons in the PPL1 cluster of *parkin* mutant flies. Data are shown as the mean ± SEM (n = 16-20 brain hemispheres per genotype), and the asterisks

indicate statistically significant values (one-way ANOVA with Bonferroni's multiple comparison test) relative to control. Datasets labelled "control" and "park25" are also used in Supplementary Fig. 7d. (**c**) Neuronal expression of *dNK* rescues the thoracic defects of *parkin* mutants. Asterisk(s) indicate statistical significance (chi-square two-tailed, 95% confidence intervals), n = 344 for park25, n = 1058 for park25;elav>dNK and n = 131 for park25;elav>Parkin. (**d**) *dNK* expression suppresses flight muscle defects observed in *parkin* mutants. Ultrastructural analysis of the indirect flight muscles showed that *dNK* expression rescues mitochondrial defects in *park25* mutants (my, myofibrils; m, mitochondria; yellow outlines, mitochondria). Percentages of indirect flight muscle mitochondria exhibiting fragmented cristae are presented for the indicated genotypes (n = 140 for control, n = 174 for park25, n = 130 for park25; elav>dNK). Asterisks indicate statistical significance (chi-square, two-tailed, 95% confidence intervals).

Supplementary Figure 6. Effects of dietary supplementation with dNs or FA in *pink1* mutants. Related to Fig. 6.

(**a**) dNs or FA enhance ATP levels in *pink1* mutants. ATP levels were measured using a bioluminescence assay. Data are shown as the mean ± SD (n = 3 in each group). Statistical significance is indicated (one-way ANOVA with Bonferroni's multiple comparison test). See Supplementary Table 9 for statistics source data. (**b**) dNs or FA do not affect dMfn levels. Whole fly lysates were analysed using the indicated antibodies.

Supplementary Figure 7. Effects of dietary supplementation with dNs or FA in *pink1* and *parkin* mutants. Related to Fig. 7.

(**a**) Percentages of indirect flight muscle mitochondria exhibiting fragmented cristae (numbers on the bar) are presented for the indicated genotypes. Asterisks indicate statistical significance (chi-square, two-tailed, 95% confidence intervals), n = 140 for control, n = 469 for pink1B9, n = 226 for pink1B9+dNs, n = 118 for pink1B9+FA. (**b**) Dietary supplementation with purine rescues the thoracic defects of *pink1* mutants more effectively than those with pyrimidines. *pink1* mutants were exposed to a purine (dG+dA) or pyrimidine (dC+dT)-supplemented diet after egg laying. *P*-values are indicated (chi-square, two-tailed, 95% confidence intervals), n = 129 for normal diet, n = 194 for purines, n = 404 for pyrimidines. (**c**) dNs or FA reverse the loss of $\Delta\psi m$ in *parkin* mutants. The $\Delta\psi m$ is represented as percentage of control. The error bars represent the mean ± SEM (n = 5-7 brains per condition). Statistical significance is indicated by asterisks (two-tailed paired *t* test). Datasets labelled "control" and "park25" are also used in Supplementary Fig. 5a (**d**) dNs or FA reverse the loss of dopaminergic neurons in the PPL1 cluster of *parkin* mutant flies. Data are shown as the mean ± SEM (n = 16-20 brain hemispheres in each group), and the asterisks indicate statistically significant values (one-way ANOVA with Bonferroni's multiple comparison test). Datasets labelled "control" and "park25" are also used in Supplementary Fig. 5b (**e**) Dietary supplementation with dNs or FA rescues the thoracic defects of *parkin* mutants. *parkin* mutants were exposed to a dNs or FA-supplemented diet after egg laying (n = 355 for normal diet, n = 96 for +dNs and n = 66 for +FA). *P*-values are indicated (chi-square two-tailed, 95% confidence intervals). (**f**) Dietary supplementation with dNs or FA rescues the flight muscle defects observed in *parkin* mutants. Ultrastructural analysis of the indirect flight muscles showed that *dNK* expression rescues mitochondrial defects in *park25* mutants (my, myofibrils; m, mitochondria; yellow outlines, mitochondria). Percentages of indirect

flight muscle mitochondria exhibiting fragmented cristae are presented for the indicated diets (n = 174 for normal diet, n = 130 for +dNs, n = 278 for +FA). Asterisks indicate statistical significance (chi-square, two-tailed, 95% confidence intervals).

Supplementary Figure 8. Analysis of RNA quality in human post-mortem brain samples. Related to Fig. 8.

Agilent 2100 Bioanalyzer digital gel of total RNA from human brains. A high-quality sample appears as two distinct bands corresponding to the 18S and 28S ribosomal RNAs. Smearing of these bands is indicative of degradation. Lanes: L, ladder; C1-C4 control brains; Y431H, A339T, C575R, *PINK1* brains carrying mutant *PINK1*. Between 300 and 350 nanograms of RNA were applied to each non-ladder lane. The asterisk indicates the sample excluded from qRT-PCR analysis due to excessive RNA degradation (low RIN score).

Supplementary Figure 9. Full scans of immunoblots shown in the main figures.

Dashed boxes correspond to the cropped areas used in the corresponding main figure.

Supplementary Table 1. Identification of transcripts positively regulated in *pink1*^{B9} mutant flies. This table is related to Figure 1.

(a) Affymetrix probe-set identificator, (b) Rank Product score, calculated as a geometric mean of fold-change ranks over the number of all possible between-chip comparisons contributing to a given between-group comparison, (c) False Discovery Rate, (d) mean Fold Change.

Supplementary Table 2. Iterative Group Analysis (iGA) on positively regulated genes in *pink1*^{B9} mutant flies. This table is related to Figure 1 and Supplementary Figure 1.

Groups of functionally related genes up-regulated in pink1 mutant flies. Groups were identified by iGA. *P*-values were calculated using the hypergeometric distribution; rank of a particular gene in the list of differentially expressed genes is created from the RP list by exclusion of genes that are not assigned to the gene ontology classes; FDR, False Discovery Rate; FC, Fold Change, calculated as an antilog of a mean log-fold-change over all possible between-chip comparisons contributing to a given between-group comparison.

Supplementary Table 3. Gene network list returned by R spider on submission of 1693 candidate genes found to be up-regulated in *pink1*^{B9} mutant flies. This table is related to Figure 1 and Supplementary Figure 1.

FDR, False Discovery Rate; FC, Fold Change; UA, genes unassigned to individual pathways.

Supplementary Table 4. List of *R* spider network components below 5% FDR threshold. This table is related to Supplementary Figure 1.

UA, genes unassigned to individual pathways by the algorithm.

Supplementary Table 5. Heat map of statistically significant biochemicals altered in *pink1*^{B9} mutant flies. This is related to Figure 1.

Shaded cells indicate p≤0.05 (red indicates that the mean values are significantly higher for that comparison; green values significantly lower). Blue-bolded text indicates 0.05<p<0.10. All data are normalized to Bradford protein assay measurements.

Supplementary Table 6. Heat map of statistically significant biochemicals altered in *pink1*^{B9} and *pink1*^{B9}*, da>dNK* mutant flies. This table is related to Figure 3.

Shaded cells indicate p≤0.05 (red indicates that the mean values are significantly higher for that comparison; green values significantly lower). Blue-bolded text indicates 0.05<p<0.10. All data are normalized to Bradford protein assay measurements.

Supplementary Table 7. Heat map of statistically significant biochemicals altered upon dietary supplementation of control and *pink1* mutant flies with either deoxyribonucleosides (dNs) or folic acid (FA). This table is related to Figure 6.

Shaded cells indicate p≤0.05 (red indicates that the mean values are significantly higher for that comparison; green values significantly lower). All data are normalized to Bradford protein assay measurements.

Supplementary Table 8. *Drosophila* genotypes

This table lists the genotypes of *Drosophila* stocks used in each individual figure.

Supplementary Table 9. Statistics source data.

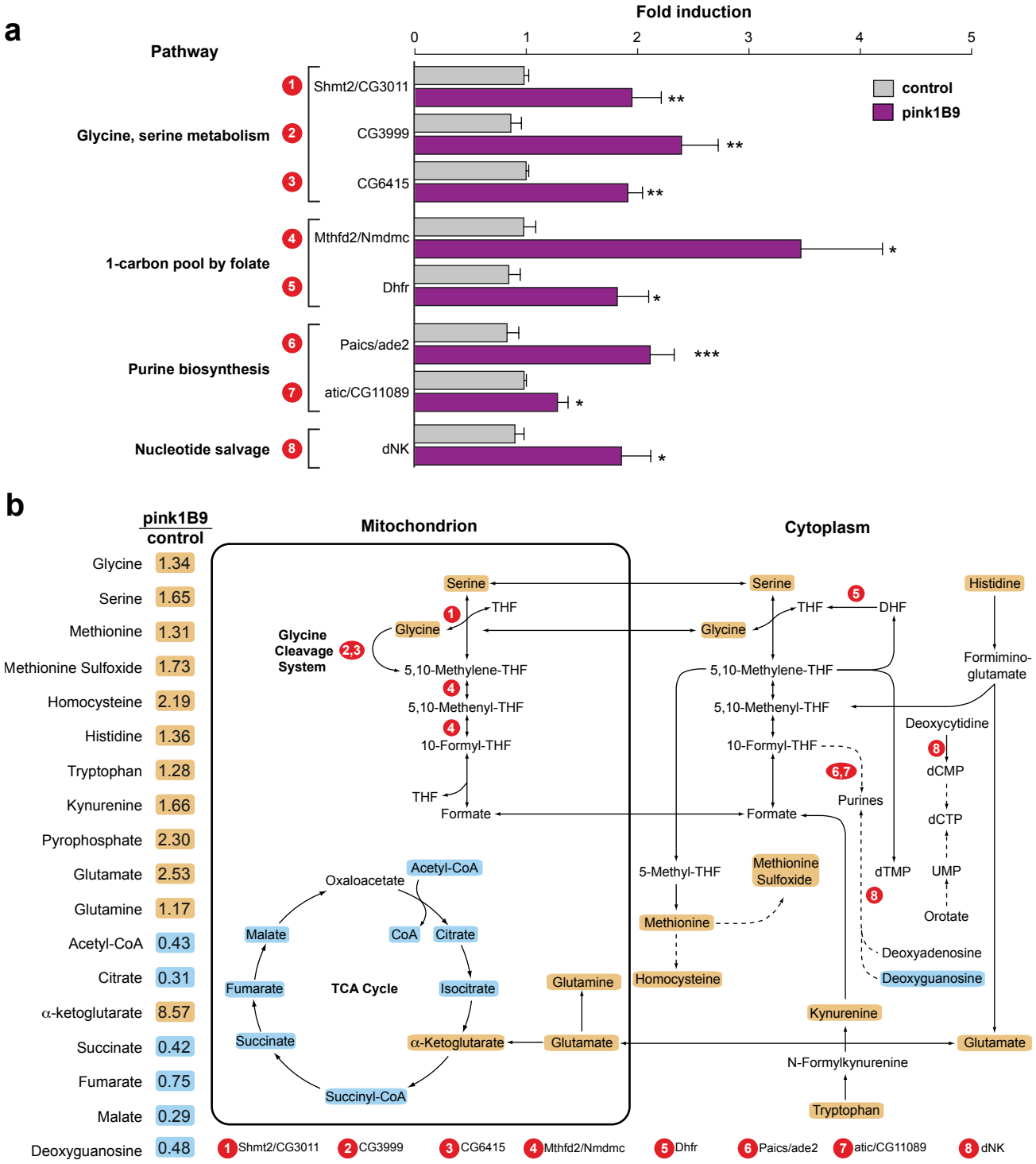
a
Fold induction
0
1
2
3
4
5
Pathway
control
pink1B9
Glycine, serine metabolism
1 Shmt2/CG3011
2 CG3999
3 CG6415
1-carbon pool by folate
4 Mthfd2/Nmdmc
5 Dhfr
Purine biosynthesis
6 Paics/ade2
7 atic/CG11089
Nucleotide salvage
8 dNK
b
pink1B9
control
Glycine 1.34
Serine 1.65
Methionine 1.31
Methionine Sulfoxide 1.73
Homocysteine 2.19
Histidine 1.36
Tryptophan 1.28
Kynurenine 1.66
Pyrophosphate 2.30
Glutamate 2.53
Glutamine 1.17
Acetyl-CoA 0.43
Citrate 0.31
α-ketoglutarate 8.57
Succinate 0.42
Fumarate 0.75
Malate 0.29
Deoxyguanosine 0.48
Mitochondrion
Cytoplasm
Glycine Cleavage System
TCA Cycle
Serine
Glycine
THF
DHF
5,10-Methylene-THF
5,10-Methenyl-THF
10-Formyl-THF
Formate
Histidine
Formimino-glutamate
Deoxycytidine
dCMP
dCTP
dTMP
UMP
Orotate
Purines
Deoxyadenosine
Deoxyguanosine
5-Methyl-THF
Methionine
Methionine Sulfoxide
Homocysteine
Kynurenine
N-Formylkynurenine
Tryptophan
Glutamate
Glutamine
α-Ketoglutarate
Acetyl-CoA
CoA
Citrate
Isocitrate
Oxaloacetate
Malate
Fumarate
Succinate
Succinyl-CoA
1 Shmt2/CG3011
2 CG3999
3 CG6415
4 Mthfd2/Nmdmc
5 Dhfr
6 Paics/ade2
7 atic/CG11089
8 dNK

Figure 1

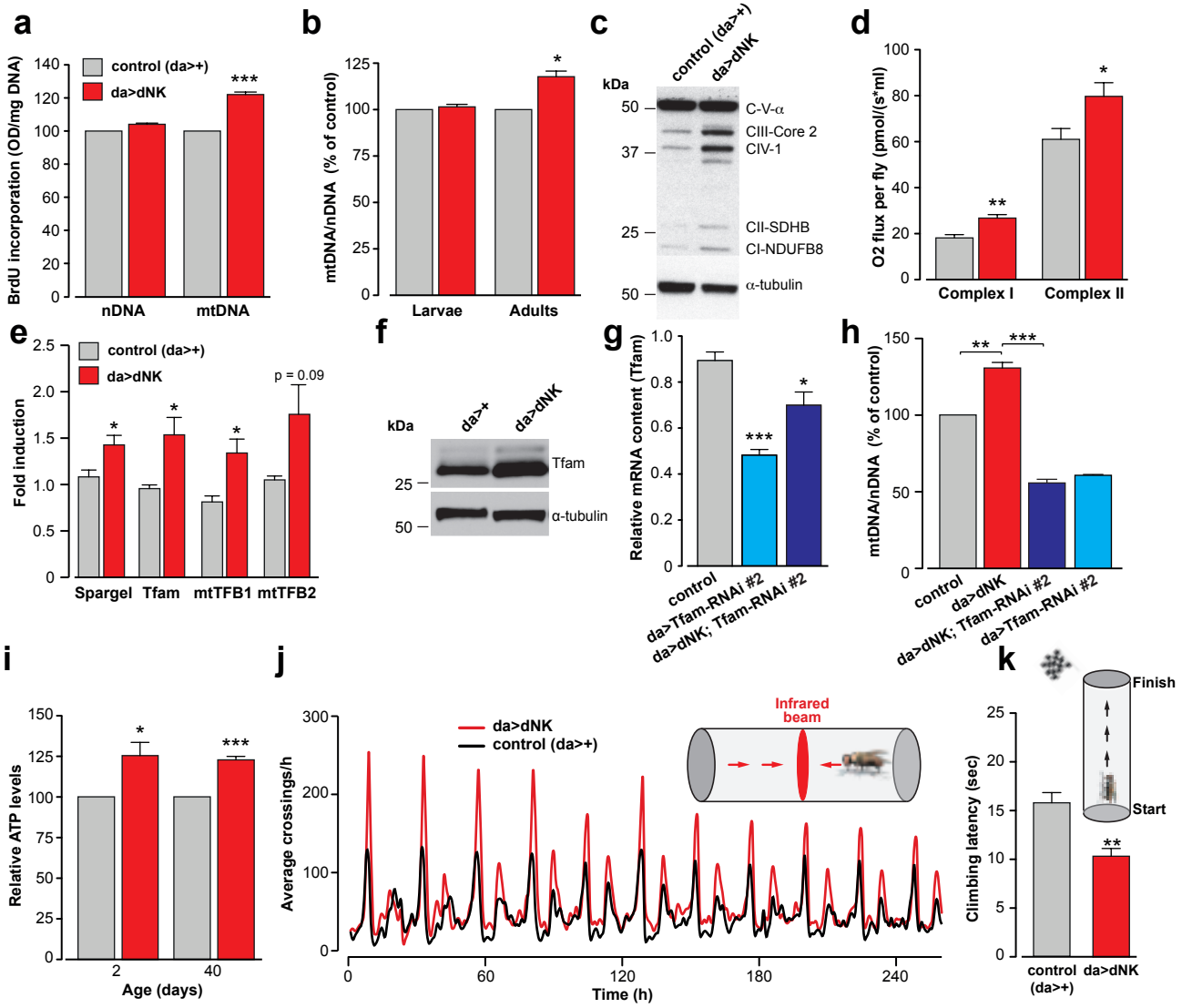
a
BrdU incorporation (OD/mg DNA)
control (da>+)
da>dNK
nDNA
mtDNA
b
mtDNA/nDNA (% of control)
Larvae
Adults
c
control (da>+)
da>dNK
kDa
C-V-α
CIII-Core 2
CIV-1
CII-SDHB
CI-NDUFB8
α-tubulin
d
O2 flux per fly (pmol/(s*ml)
Complex I
Complex II
e
Fold induction
p = 0.09
Spargel
Tfam
mtTFB1
mtTFB2
f
kDa
da>+
da>dNK
Tfam
α-tubulin
g
Relative mRNA content (Tfam)
control
da>Tfam-RNAi #2
da>dNK; Tfam-RNAi #2
h
mtDNA/nDNA (% of control)
control
da>dNK
da>dNK; Tfam-RNAi #2
da>Tfam-RNAi #2
i
Relative ATP levels
Age (days)
j
Average crossings/h
da>dNK
control (da>+)
Infrared beam
Time (h)
k
Finish
Start
Climbing latency (sec)
control (da>+)
da>dNK

Figure 2

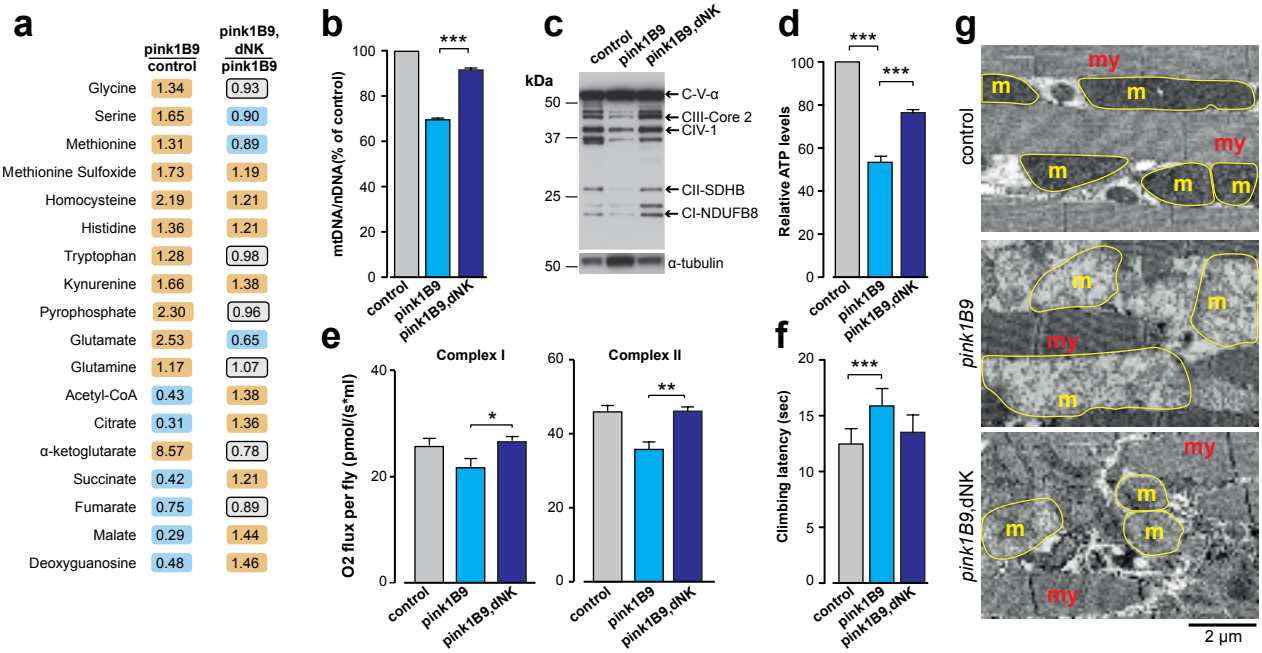
a
pink1B9 control
pink1B9, dNK pink1B9
Glycine 1.34 0.93
Serine 1.65 0.90
Methionine 1.31 0.89
Methionine Sulfoxide 1.73 1.19
Homocysteine 2.19 1.21
Histidine 1.36 1.21
Tryptophan 1.28 0.98
Kynurenine 1.66 1.38
Pyrophosphate 2.30 0.96
Glutamate 2.53 0.65
Glutamine 1.17 1.07
Acetyl-CoA 0.43 1.38
Citrate 0.31 1.36
α-ketoglutarate 8.57 0.78
Succinate 0.42 1.21
Fumarate 0.75 0.89
Malate 0.29 1.44
Deoxyguanosine 0.48 1.46
b
mtDNA/nDNA(% of control)
control
pink1B9
pink1B9,dNK
c
kDa
C-V-α
CIII-Core 2
CIV-1
CII-SDHB
CI-NDUFB8
α-tubulin
d
Relative ATP levels
e
Complex I
Complex II
O2 flux per fly (pmol/(s*ml)
f
Climbing latency (sec)
g
control
pink1B9
pink1B9,dNK
m
my
2 µm

Figure 3

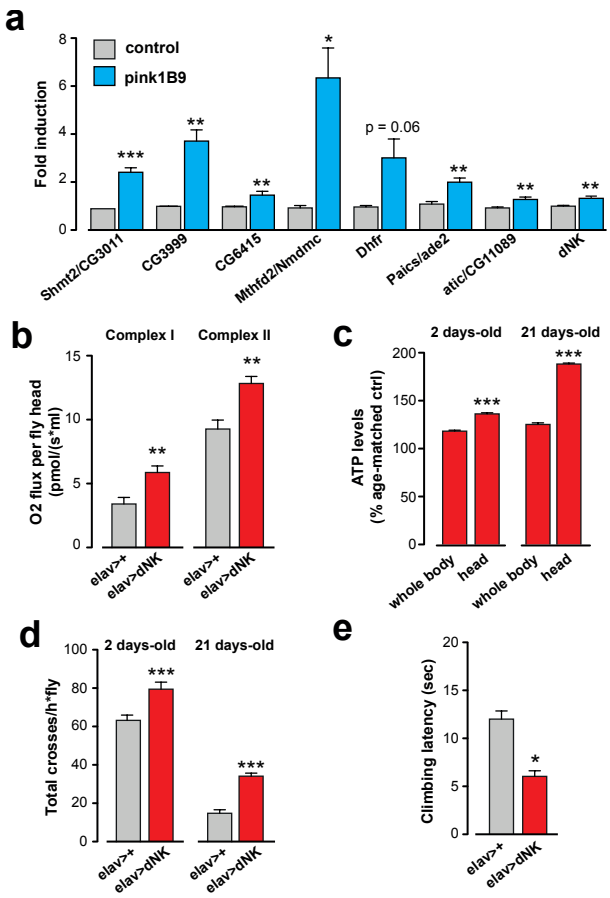
a
control
pink1B9
Fold induction
p = 0.06
Shmt2/CG3011
CG3999
CG6415
Mthfd2/Nmdmc
Dhfr
Paics/ade2
atic/CG11089
dNK
b
Complex I
Complex II
O2 flux per fly head (pmol/(s*ml)
elav>+
elav>dNK
c
2 days-old
21 days-old
ATP levels (% age-matched ctrl)
whole body
head
d
Total crosses/h*fly
e
Climbing latency (sec)

Figure 4

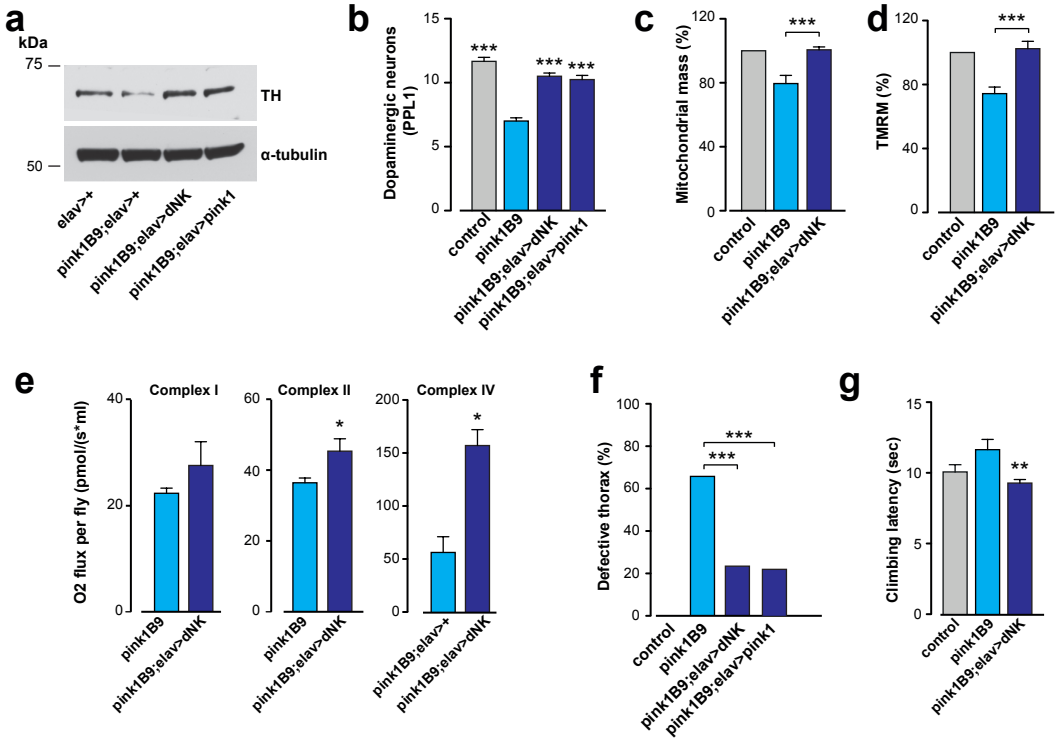
a
kDa
75
50
TH
α-tubulin
elav>+
pink1B9;elav>+
pink1B9;elav>dNK
pink1B9;elav>pink1
b
Dopaminergic neurons (PPL1)
***
***
***
control
pink1B9
pink1B9;elav>dNK
pink1B9;elav>pink1
c
Mitochondrial mass (%)
***
control
pink1B9
pink1B9;elav>dNK
d
TMRM (%)
***
control
pink1B9
pink1B9;elav>dNK
e
O2 flux per fly (pmol/(s*ml)
Complex I
Complex II
Complex IV
*
*
pink1B9
pink1B9;elav>dNK
pink1B9;elav>+
pink1B9;elav>dNK
f
Defective thorax (%)
***
***
control
pink1B9
pink1B9;elav>dNK
pink1B9;elav>pink1
g
Climbing latency (sec)
**
control
pink1B9
pink1B9;elav>dNK

Figure 5

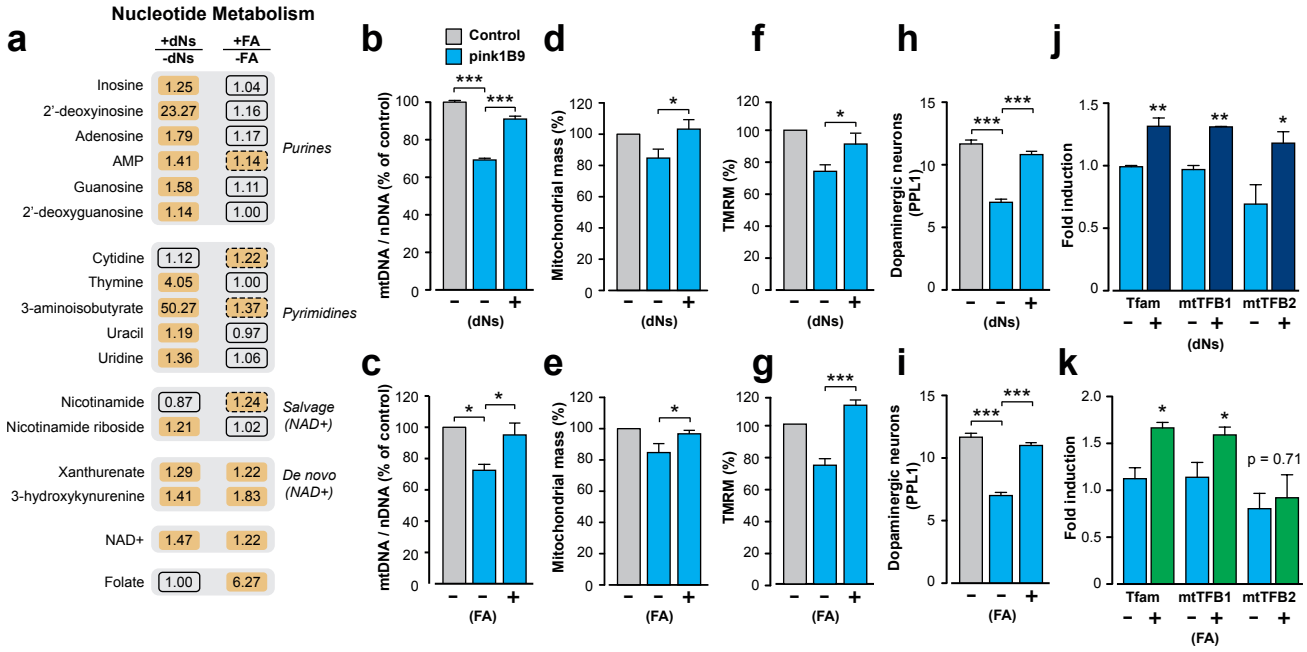
Nucleotide Metabolism
a
+dNs / -dNs
+FA / -FA
Inosine 1.25 1.04
2'-deoxyinosine 23.27 1.16
Adenosine 1.79 1.17
AMP 1.41 1.14
Guanosine 1.58 1.11
2'-deoxyguanosine 1.14 1.00
Purines
Cytidine 1.12 1.22
Thymine 4.05 1.00
3-aminoisobutyrate 50.27 1.37
Uracil 1.19 0.97
Uridine 1.36 1.06
Pyrimidines
Nicotinamide 0.87 1.24
Nicotinamide riboside 1.21 1.02
Salvage (NAD+)
Xanthurenate 1.29 1.22
3-hydroxykynurenine 1.41 1.83
De novo (NAD+)
NAD+ 1.47 1.22
Folate 1.00 6.27
b
Control
pink1B9
mtDNA / nDNA (% of control)
(dNs)
c
(FA)
d
Mitochondrial mass (%)
e
f
TMRM (%)
g
h
Dopaminergic neurons (PPL1)
i
j
Fold induction
Tfam
mtTFB1
mtTFB2
k
p = 0.71

Figure 6

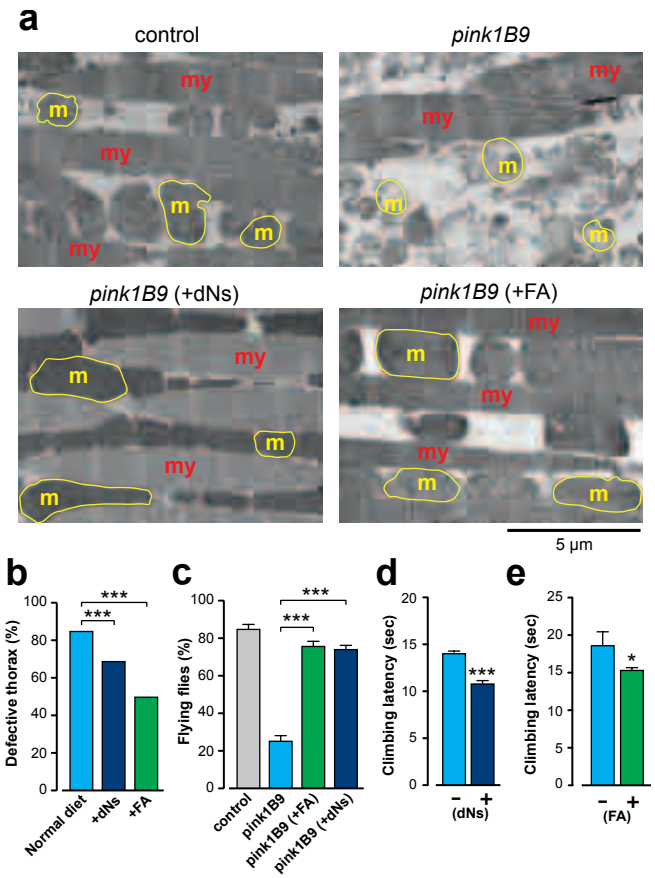
a
control
pink1B9
pink1B9 (+dNs)
pink1B9 (+FA)
my
m
5 μm
b
Defective thorax (%)
Normal diet
+dNs
+FA
c
Flying flies (%)
control
pink1B9
pink1B9 (+FA)
pink1B9 (+dNs)
d
Climbing latency (sec)
(dNs)
e
Climbing latency (sec)
(FA)

Figure 7

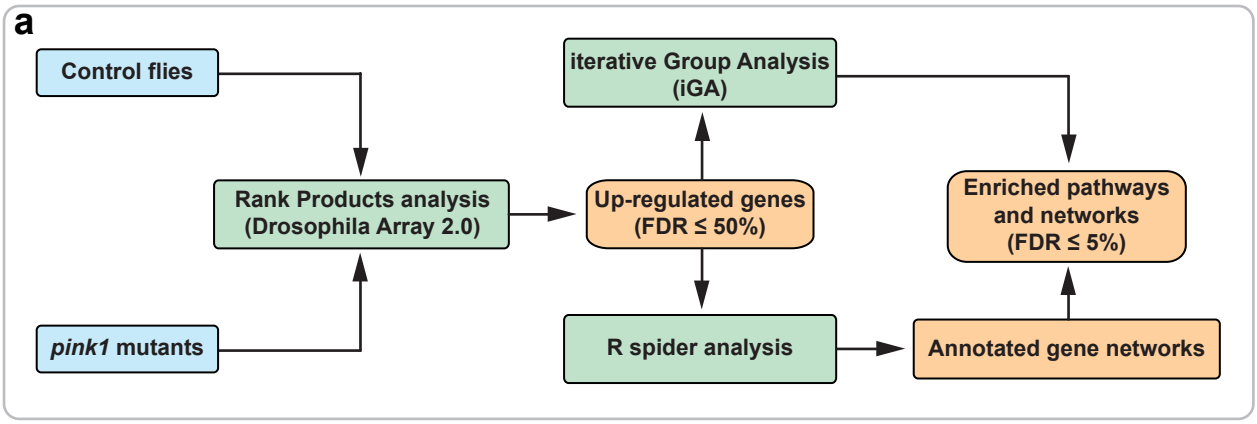

b

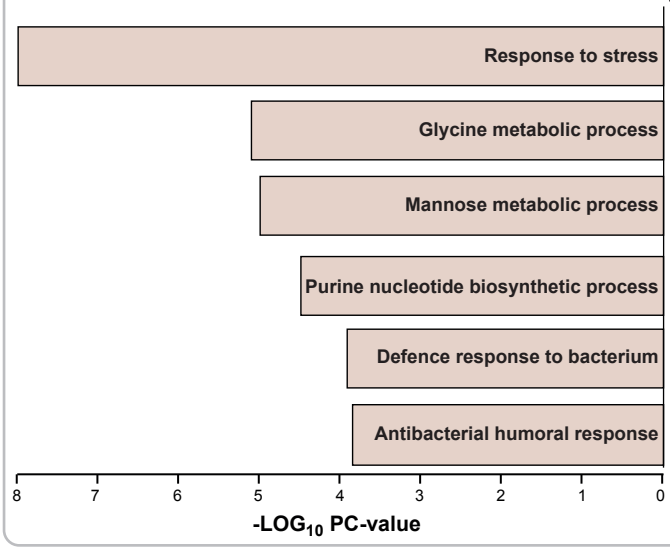

Pathway	*P*-value	Rank	Entrez	Gene Symbol	FDR	FC
1	6.00E-03	1	44921	Hsp70Ba	0	23.6
	3.60E-05	2	44920	Hsp70Aa	0	21.6
	8.20E-07	4	3771872	Hsp22	0	13.6
	5.90E-09	5	48583	Hsp70Bc	0	15.2
2	2.20E-03	12	41253	CG3999	0	4.1
	9.60E-06	34	31524	CG3011	0.39	2.4
3	1.10E-02	15	34203	CG9463	0	3.8
	2.30E-04	32	34204	CG9465	0.36	2.5
	1.40E-05	69	34205	CG9466	0.89	2.1
4	2.70E-02	30	33986	ade3	0.38	2.5
	4.50E-04	35	42973	CG11089	0.41	2.4
	4.30E-05	79	33847	ade2	0.89	2.0
5	1.10E-02	6	38122	LysX	0	8.3
	1.40E-04	10	36708	Mtk	0	4.2
6	2.40E-02	10	36708	Mtk	0	4.2
	4.30E-04	13	37099	IM23	0	3.7
	1.50E-04	44	38419	Drs	0.47	2.6

c

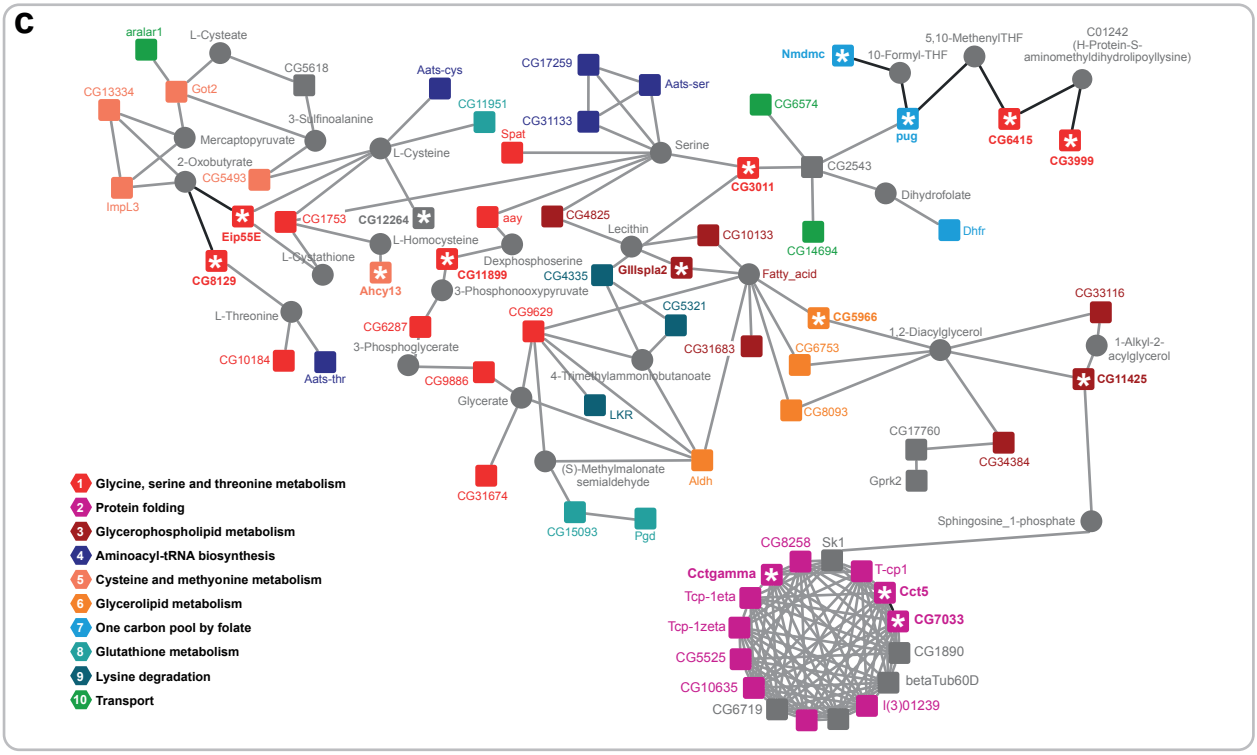

Supplementary Figure 1

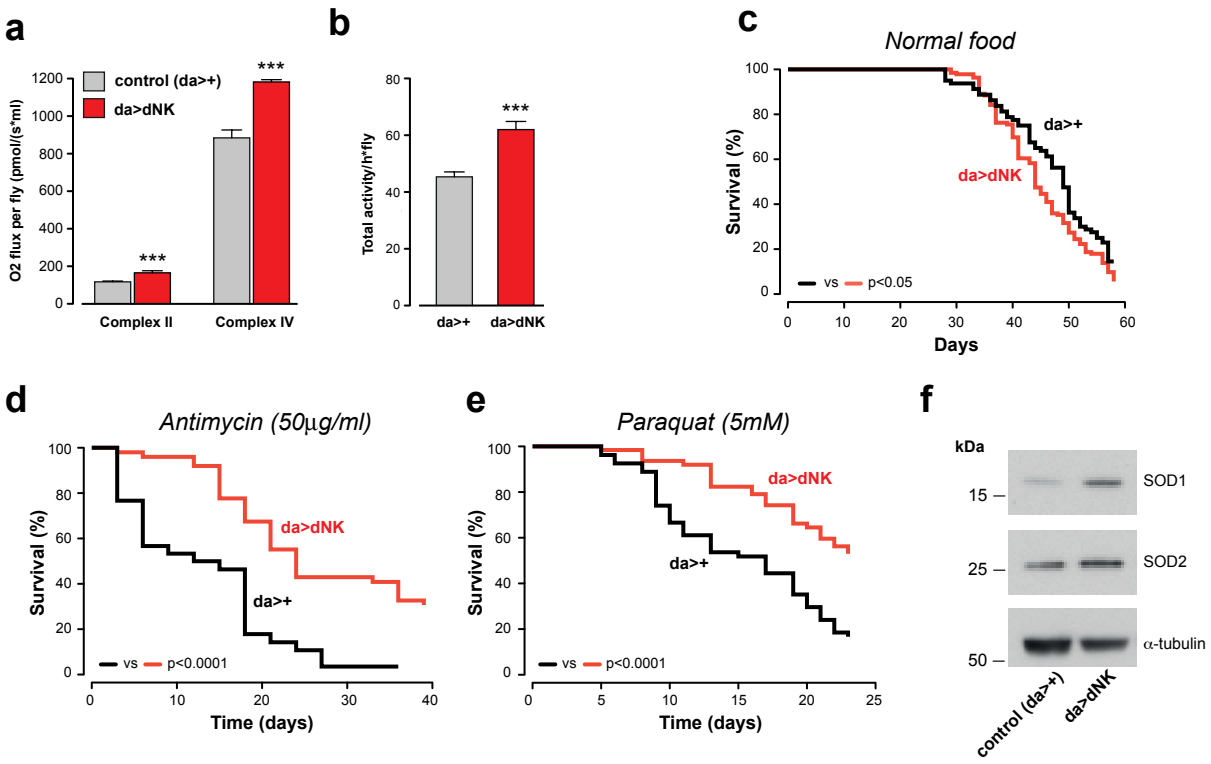

Supplementary Figure 2

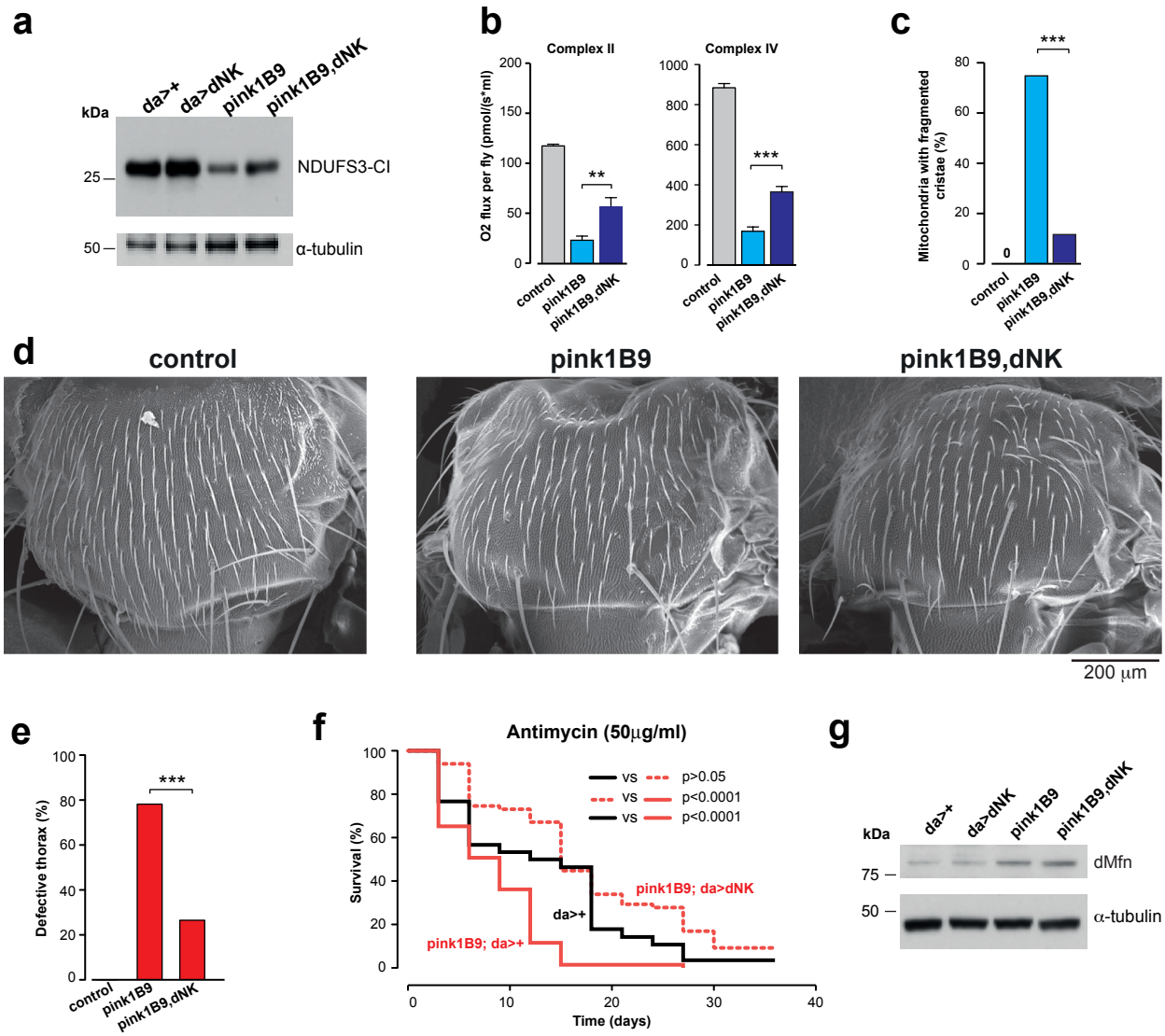

Supplementary Figure 3

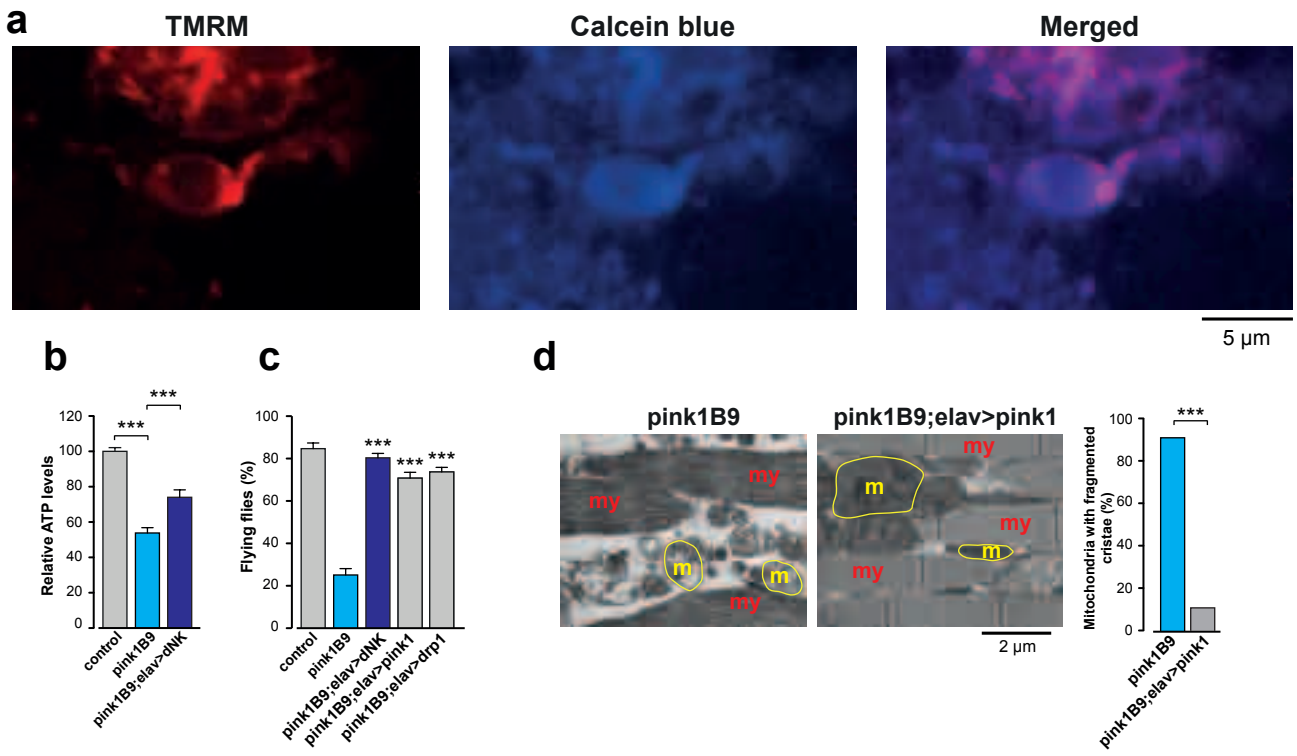

Supplementary Figure 4

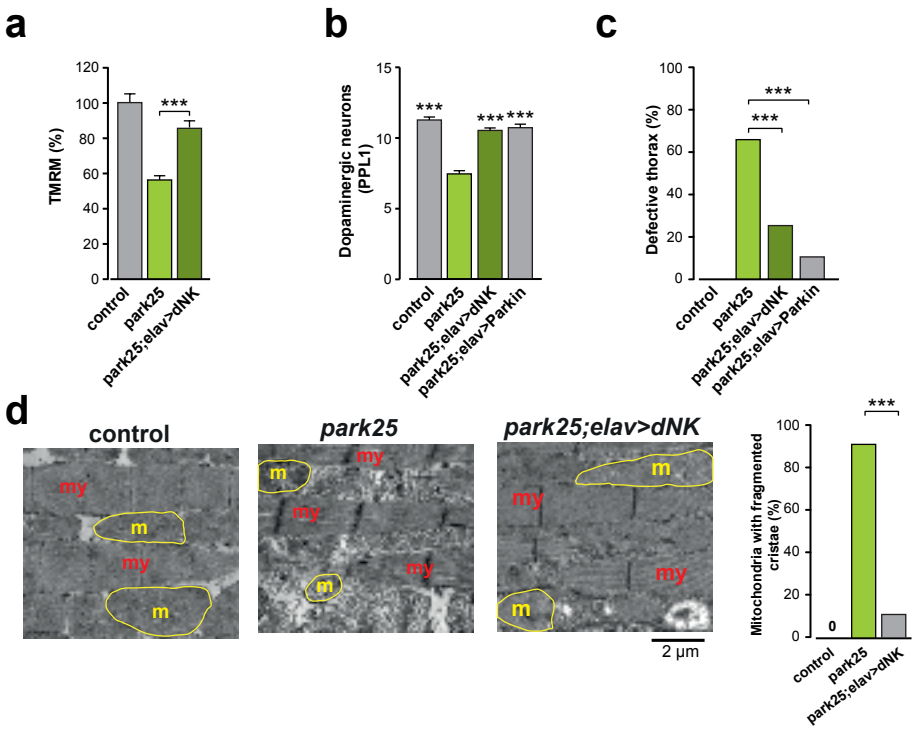

Supplementary Figure 5

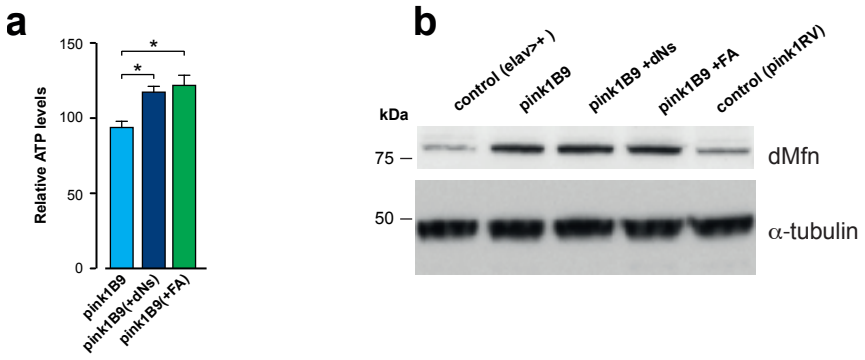

Supplementary Figure 6

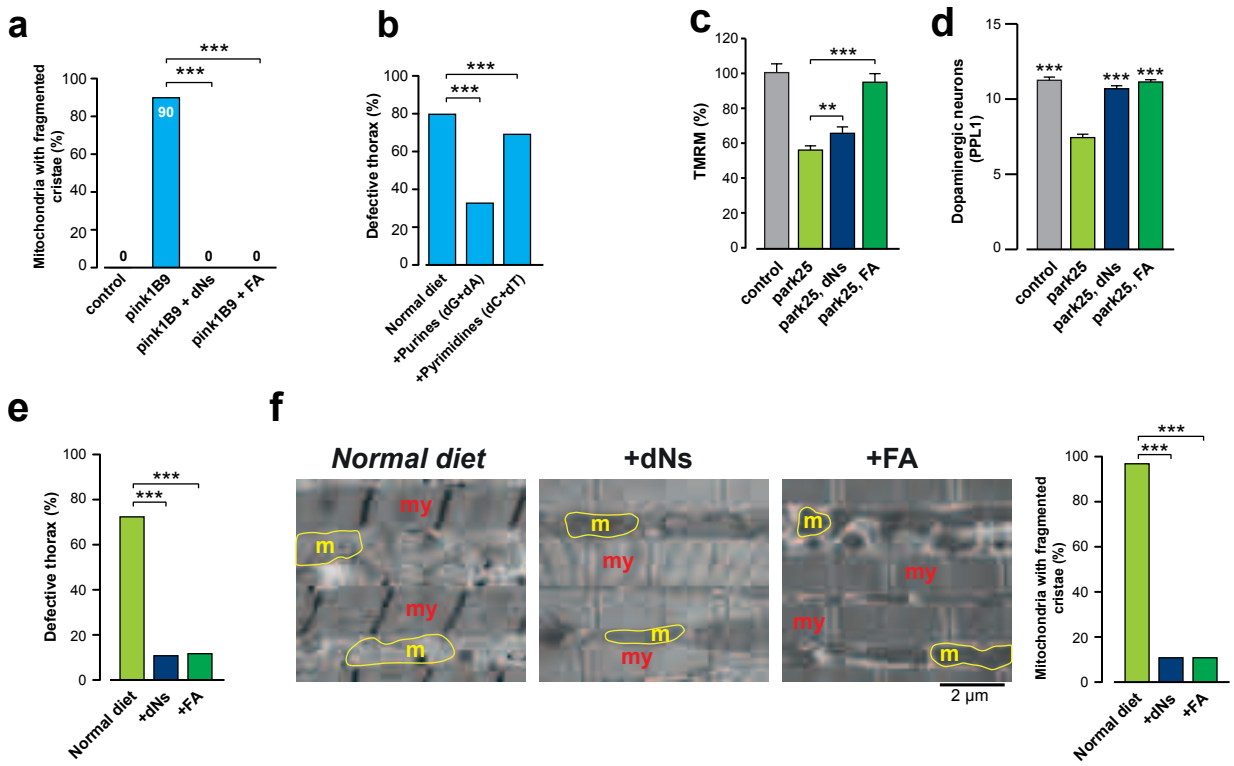

Supplementary Figure 7

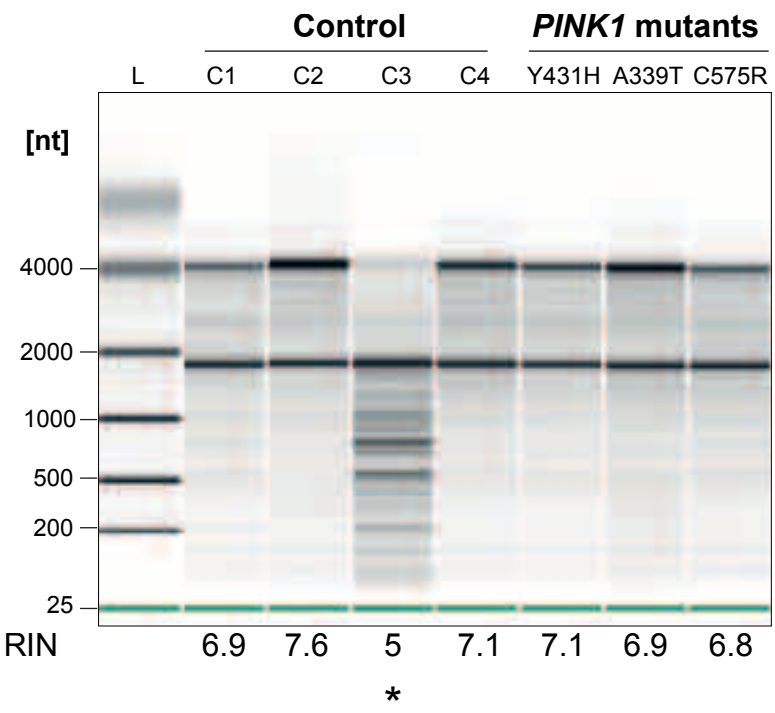

Supplementary Figure 8

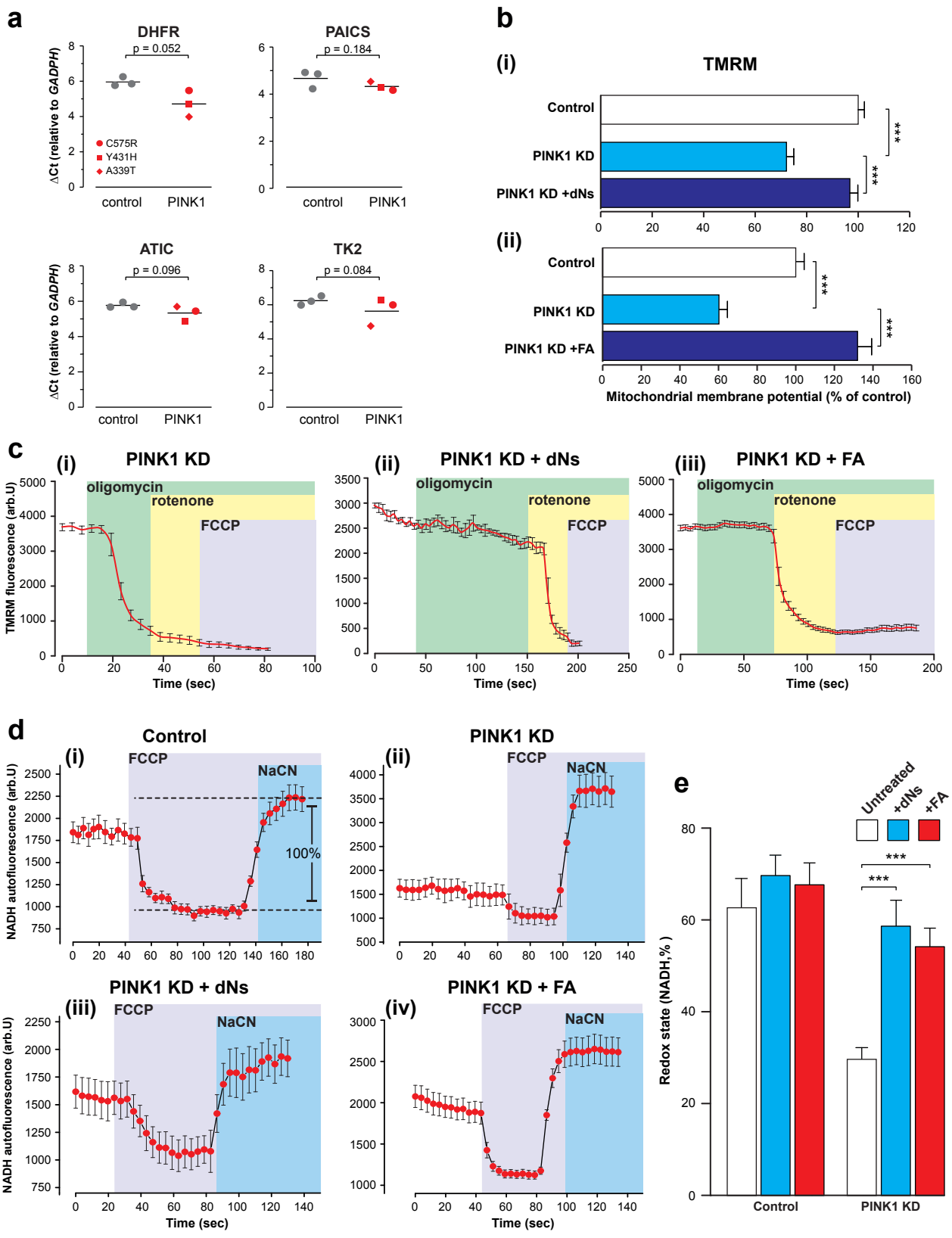
a
DHFR
p = 0.052
PAICS
p = 0.184
ATIC
p = 0.096
TK2
p = 0.084
ΔCt (relative to GADPH)
C575R
Y431H
A339T
control
PINK1
b
(i)
TMRM
Control
PINK1 KD
PINK1 KD +dNs
(ii)
PINK1 KD +FA
Mitochondrial membrane potential (% of control)
c
(i) PINK1 KD
(ii) PINK1 KD + dNs
(iii) PINK1 KD + FA
oligomycin
rotenone
FCCP
TMRM fluorescence (arb.U)
Time (sec)
d
Control
PINK1 KD
PINK1 KD + dNs
PINK1 KD + FA
NaCN
100%
NADH autofluorescence (arb.U)
e
Untreated
+dNs
+FA
Redox state (NADH,%)

Figure 8

Figure 2c

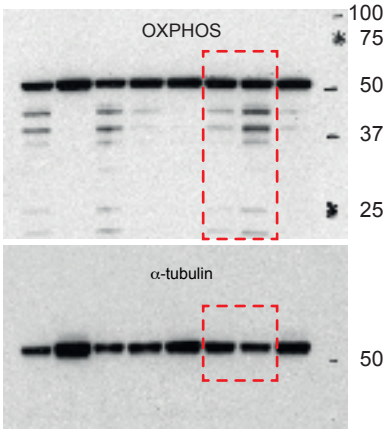

Figure 2f

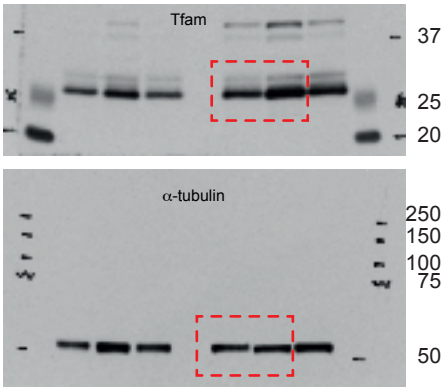

Figure 3c

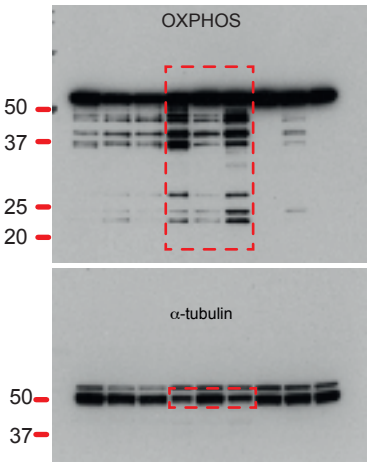

Figure 5a

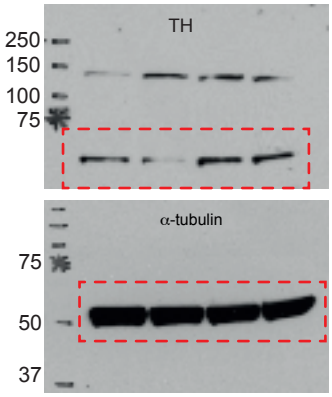

Supplementary Figure 9